CLASSIFICATION OF TIGHT CONTACT STRUCTURES ON THE WEEKS MANIFOLD

A Dissertation
Presented to
The Academic Faculty

By

Hyunki Min

In Partial Fulfillment
of the Requirements for the Degree
Doctor of Philosophy in the
School of Mathematics
College of Science

Georgia Institute of Technology

August 2021

CLASSIFICATION OF TIGHT CONTACT STRUCTURES ON THE WEEKS MANIFOLD

Thesis committee:

Dr. John Etnyre
School of Mathematics
Georgia Institute of Technology

Dr. Dan Margalit
School of Mathematics
Georgia Institute of Technology

Dr. Mohammad Ghomi
School of Mathematics
Georgia Institute of Technology

Dr. Ko Honda
School of Mathematics
University of California, Los Angeles

Dr. Jennifer Hom
School of Mathematics
Georgia Institute of Technology

Date approved: Aril 23, 2021

To my parents

ACKNOWLEDGMENTS

I would like to thank my advisor John Etnyre for his help, support, and patience. Because of his guidance, I could finish this thesis. I also appreciate the helpful discussions with James Conway that led to some of the results of this thesis. I am also grateful to my committee, Ko Honda, Jen Hom, Dan Margalit, and Mohammad Ghomi, from whom I received a lot of advice and support.

I am grateful to my fellow graduate students for their friendship and mathematical discussions: Anubhav Mukherjee, Agniva Roy, Surena Hozoori, Sudipta Kolay, Andrew McCullough, Jiaqi Yang, Christina Giannitsi, Jaemin Park, Kisun Lee, Bhanu Kumar, Jaewoo Jung, Jieun Seong, Hongyi Zhou and many others.

Finally, I would like to thank my family for their love and support.

TABLE OF CONTENTS

Acknowledgments iv

List of Figures vii

Chapter 1: Introduction 1

Chapter 2: Contact Topology Preliminaries 3

2.1 Convex surfaces 3

2.2 Basic slices and solid tori 8

2.3 Contact surgery and Heegaard Floer homology 9

2.4 Spin^c structure 11

Chapter 3: Constructing contact structures via surgery 13

Chapter 4: An upper bound on tight contact structures 19

4.1 A Rational open book decomposition 19

4.2 Twisting $\leqslant$ -1 24

4.3 Finding tight contact structures 33

4.4 Bypass case 39

4.5 Twisting $\geqslant 0$ 41

4.6 Thickening the solid torus 42

References 50

LIST OF FIGURES

1.1 The Weeks manifold 2

2.1 A standard convex torus with two dividing curves. The top and bottom sides are identified, as are the left and right sides. The dashed black lines represent dividing curves. The red lines represent Legendrian ruling curves and the Black solid lines represent Legendrian divides. 5

2.2 The standard model of intersection between two convex surfaces. 5

2.3 Rounding an edge between two convex surfaces. 6

2.4 Bypass attachments 6

2.5 The Farey graph 7

3.1 The result of left-handed Rolfsen twist on K_1 13

3.2 The result of blow-ups 14

3.3 Legendrian realization of the link in Figure 3.2 14

3.4 Another surgery diagram for the Weeks manifold. 15

3.5 Legendrian realization of the third link in Figure 3.4. 15

3.6 Returning back to the Whitehead link 17

4.1 The bundle structure of $M = S^3 \backslash N$. Opposite rectangles are identified. The top and bottom are glued by ψ. 20

4.2 List of possible bypass attachments for Case III(a) with $n = 3$. The top and bottom are identified as are the left and right sides. The dashed lines represent dividing curves and the blue solid lines represent the attachment for the bypasses. The bypasses are attached from the back. For (A), (B) and (C), the slope of bypass attachment is less than 0. For (D), the slope of the bypass attachment is between 0 and 1. 25

4.3 Continuation of list of possible bypass attachments for Case III(a) with $n = 3$. For (E) and (F), the slope of bypass attachment is between 0 and 1. For (G), (H) and (I), the slope of bypass attachment is between 1 and ∞. . . 26

4.4 Two possible bypass attachment for Case I(a) with $n = 3, m = 1$. 27

4.5 The left and right sides are identified. The dashed lines represent dividing curves. The top and bottom parts are neighborhoods of $\partial\Sigma_i$ in Σ_i and the middle part is the region $\partial\Sigma \times I$. The shaded regions are the result of edge-rounding. The dividing curves on Σ_i divide $\partial\Sigma_i$ into six intervals and they are labeled 1 to 6. 31

4.6 The dashed lines represent dividing curves on Σ_1 and Σ_0. The blue solid lines represent the intersection of the compressing disks D_1, D_2 with Σ_1 and Σ_0. 31

4.7 The dashed lines represent dividing curves on Σ_1 and Σ_0. The blue solid lines represent the intersection of the compressing disks D_1, D_2 with Σ_1 and Σ_0. 32

4.8 The left and right sides are identified. The dashed lines represent dividing curves. The top and bottom parts are neighborhoods of $\partial\Sigma_i$ in Σ_i and the middle part is the region $\partial\Sigma \times I$. The shaded regions are the result of edge-rounding. The dividing curves on Σ_i divide $\partial\Sigma_i$ into two intervals and they are labeled 1 and 2 respectively. 34

4.9 The dashed lines represent dividing curves on Σ_1 and Σ_0. The blue solid lines represent the intersection of the compressing disks with Σ_1 and Σ_0. . . 35

4.10 The dashed lines represent dividing curves on Σ_1 and Σ_0. The blue solid lines represent the intersection of the compressing disk with Σ_1 and Σ_0. . . 36

4.11 The dashed lines represent dividing curves on Σ_1 and Σ_0. The blue solid lines represent the intersection of the compressing disk with Σ_1 and Σ_0. . . 37

4.12 The dashed lines represent dividing curves on the compressing disk D. The blue dots represent the intersection points of D and Γ_1 and the red dots represent the intersection points of D and Γ_0. 37

4.13 The dashed lines represent dividing curves on Σ_1 and Σ_0. The blue solid lines represent the intersection of the compressing disks with Σ_1 and Σ_0. . . 39

4.14 Gluing two tight contact structures. 40

4.15 List of possible bypass attachments for Case III(a) with $n > 3$. The top and bottom are identified as are the left and right sides. The dashed lines represent dividing curves and the blue solid lines represent the attachment for the bypasses. The bypasses are attached from the back. 43

4.16 Continuation of list of possible bypass attachments for Case III(a) with $n > 3$. 44

4.17 Two possible bypass attachments for Case I(a) with $n = 3, m = 1$. 45

4.18 The dashed lines represent dividing curves on Σ_1 and Σ_0. The blue solid lines represent the intersection of the compressing disk D with Σ_1 and Σ_0 . 48

4.19 The dashed lines represent dividing curves on the compressing disk D. The red dots represent the intersection points of D and the dividing arcs in Γ_0. The green dot represents the intersection point of D and the closed dividing curve in Γ_0. 48

4.20 The dashed lines represent dividing curves on Σ_1 and Σ_0. The blue solid lines represent the intersection of the compressing disk D with Σ_1 and Σ_0 . 49

CHAPTER 1
INTRODUCTION

A co-orientable contact 3-manifold (M, ξ) is *overtwisted* if it contains an overtwisted disk, which is an embedded disk tangent to the contact planes along the boundary, and *tight* if it does not contain an overtwisted disk. In [1], Eliashberg classified overtwisted contact structures. Hence, more recent studies focus on the classification of tight contact structures.

Since tight contact structures respect the prime decomposition of 3-manifolds, it is only necessary to consider the classification of tight contact structures on prime manifolds. Geometrization of 3-manifolds implies that a prime 3-manifold is either Seifert fibered, toroidal or hyperbolic. For Seifert fibered manifolds, there have been several results. For lens spaces including $S^3, S^1 \times S^2$, tight contact structures were classified in [2, 3, 4, 5]. Furthermore, after Etnyre and Honda showed that there exists no tight contact structure on the Poincaré homology sphere with reversed orientation $-\Sigma(2,3,5)$ in [6], there have been several classification results on some Seifert fibered spaces. For example, see [7, 8, 9]. For toroidal manifolds, we can construct infinitely many tight contact structures by using Giroux torsion. Tight contact structures on T^3 were classified in [10, 11]. Later on, Giroux and Honda independently classified tight contact structures on torus bundles over a circle in [4, 12] and [13]. In [14, 15], it was shown that a closed orientable irreducible 3-manifold carries infinitely many tight contact structures up to isotopy if and only if it is toroidal.

For hyperbolic manifolds, much less is known. In [16], Honda, Kazez and Matić classified tight contact structures on genus 2 surface bundles over a circle when they have an extremal relative Euler class. In [17], Conway and the author classified tight contact structures on surgeries on the figure-8 knot. However, none of them is an L-space. In this thesis, we will classify tight contact structures on the Weeks manifold, which is a hyperbolic L-space, obtained by $(5, \frac{5}{2})$-surgery on the Whitehead link. See Figure 1.1. In [18], it was

shown that the Weeks manifold has the smallest volume among closed oriented hyperbolic 3–manifolds. The existence of tight contact structures on the Weeks manifold was already shown in [19, 20, 21].

Theorem 1.0.1. *The Weeks manifold supports seven tight contact structures up to isotopy, distinguished by their Heegaard Floer contact classes.*

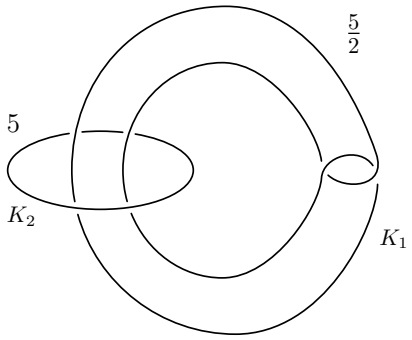

Figure 1.1: The Weeks manifold

We will prove Theorem 1.0.1 by constructing seven tight contact structures via contact surgery and distinguish them using contact classes in Heegaard Floer homology. In [21], Stipsicz used contact surgery and Heegaard Floer homology to find four tight contact structures on the Weeks manifold. We will expand this result by constructing three additional tight contact structures. After that, we will find an upper bound of tight contact structures using convex decompositions to show that there are at most seven tight contact structures on the Weeks manifold.

CHAPTER 2

CONTACT TOPOLOGY PRELIMINARIES

In this section we will briefly review several notions and theorems from contact topology which will be used throughout the paper. We assume the reader is familiar with basic contact topology at the level of [22, 23].

2.1 Convex surfaces

Here, we will review the theory of convex surfaces. For more details, see [24, 5].

Let (M, ξ) be a contact 3-manifold. We call a vector field v a *contact vector field* if its flow preserves ξ. A surface Σ (with or without boundary) is called *convex* if there exists a contact vector field transverse to Σ.

Let Σ be a surface in (M, ξ) and $\mathcal{F}$ be a characteristic foliation on Σ induced by ξ. A multi-curve Γ is called a *dividing set* of $\mathcal{F}$ if

- $\Sigma \backslash \Gamma = \Sigma_+ \sqcup \Sigma_-$.
- Γ is transverse to $\mathcal{F}$.
- there is a volume form ω on Σ and a vector field w such that
  - $\pm \mathcal{L}_w \omega > 0$ on $\Sigma_\pm$,
  - w directs $\mathcal{F}$, and
  - w points transversely out of Σ_+ along Γ.

A dividing set gives an easy criteria for checking a given surface is a convex surface.

Theorem 2.1.1 (Giroux [25])**.** *If Σ is an orientable surface in (M, ξ) with Legendrian boundary (or empty), then Σ is convex if and only if its characteristic foliation has dividing curves.*

We denote the twisting number of contact framing along a curve γ with respect to a given framing F by $tw(\gamma, F)$.

Theorem 2.1.2 (Giroux [25]). *A closed surface Σ in (M, ξ) is C^∞-close to a convex surface. If Σ has Legendrian boundary with $tw(\partial\Sigma, \Sigma) \leqslant 0$, then Σ can be C^0-perturbed in a neighborhood of the boundary and C^∞-perturbed on its interior to be convex.*

Thus, convex surfaces are generic. There is also an easy way to compute the twisting number of a simple closed Legendrian curve with respect to a given surface framing.

Theorem 2.1.3 (Kanda [10]). *Let γ be a Legendrian closed curve on a convex surface Σ with a dividing set Γ. Then,*

$$tw(\gamma, \Sigma) = -\frac{|\gamma \cap \Gamma|}{2}$$

Let Σ be a convex surface with a dividing set Γ. We call a properly embedded graph G in Σ *non-isolating* if G intersect Γ transversely and every component of $\Sigma \backslash G$ intersects Γ.

Theorem 2.1.4 (Legendrian realization principle: Honda [5]). *If G is a properly embedded non-isolating graph on a convex surface Σ, then there is an isotopic copy of Σ relative to its boundary such that G is Legendrian.*

In particular, if $\Sigma \backslash G$ is connected, G can always be realized as a Legendrian graph. This implies any non-separating curve on Σ can be realized as a Legendrian curve.

Let L be a Legendrian knot in (M, ξ). A *standard neighborhood* N of L is a tubular neighborhood of L which has a convex boundary with 2 closed dividing curves. By Theorem 2.1.1, we can arrange the characteristic foliation to be linear as shown in Figure 2.1. The singular lines parallel to dividing curves are called *Legendrian divides* and non-singular curves are called *ruling curves*. By Theorem 2.1.1 again, ruling curves can have any slope except for the slope of the dividing curves.

Now we will review how to glue two convex surfaces. Kanda [10] and Honda [5] showed that if two convex surfaces intersect along a Legendrian curve L, we have a *standard model* for this intersection. See Figure 2.2. Honda [5] used this model to glue two

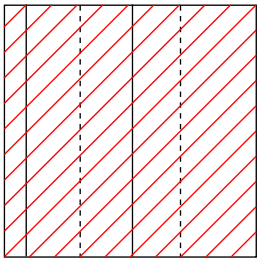

Figure 2.1: A standard convex torus with two dividing curves. The top and bottom sides are identified, as are the left and right sides. The dashed black lines represent dividing curves. The red lines represent Legendrian ruling curves and the Black solid lines represent Legendrian divides.

convex surfaces with common Legendrian boundary and get a new connected convex surface. See Figure 2.3. This is called an *edge rounding*.

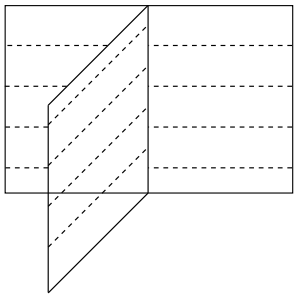

Figure 2.2: The standard model of intersection between two convex surfaces.

We can modify a dividing set in a systematical way. Let Σ be an oriented convex surface with a dividing set Γ and D be a disk with Legendrian boundary with $tb(\partial D) = -1$. Suppose $\alpha = D \cap \Sigma$ intersects Γ in three points $\{p, q, r\}$ and $\partial\alpha = \{p, q\}$ are elliptic singularity of D. By Theorem 2.1.1, we can perturb D for q to be a unique hyperbolic singularity. We call D a *bypass* and the sign of the hyperbolic singularity is called the *sign* of a bypass.

Honda proved in [5] that there is a one-sided neighborhood $\Sigma \times [0, 1]$ of $\Sigma \times \{0\} \cup D$ such that $\Sigma \times \{0, 1\}$ is convex and the dividing set on $\Sigma \times \{1\}$ is modified as shown in Figure 2.4. We say $\Sigma \times \{1\}$ is obtained from $\Sigma \times \{0\}$ by a bypass attachment along α "from

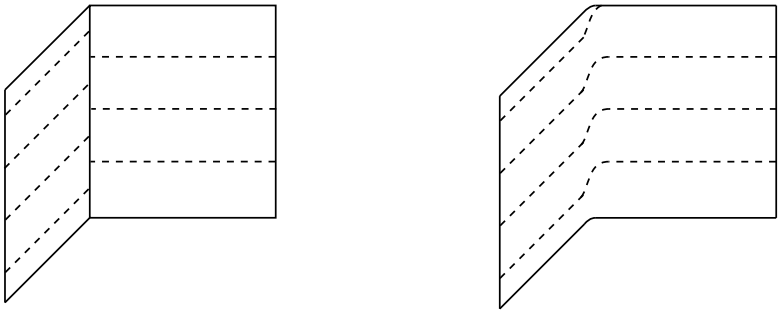

Figure 2.3: Rounding an edge between two convex surfaces.

the front". If $\Sigma \times [0,1]$ is a neighborhood of $\Sigma \times \{1\} \cup D$, then we say $\Sigma \times \{0\}$ is obtained from $\Sigma \times \{1\}$ by a bypass attachment "from the back".

Remark 2.1.5. If p and q are a same point, we obtain a *degenerate bypass*. In [5], Honda showed that this bypass still can be attached and have a similar effect as regular bypasses.

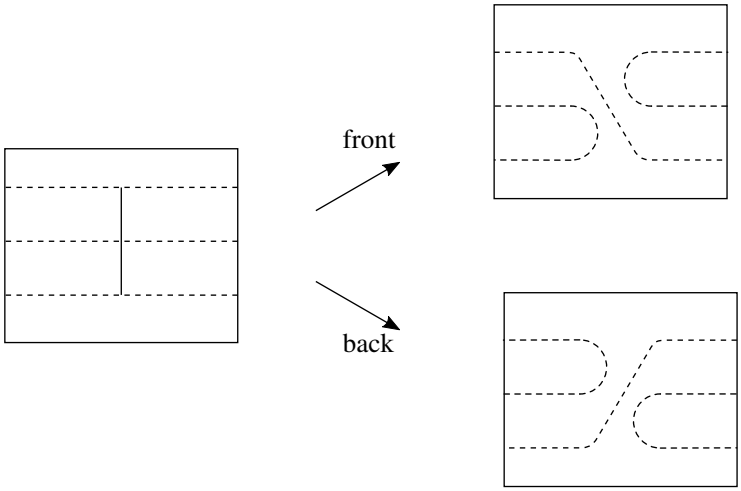

Figure 2.4: Bypass attachments

Let us investigate the effect of bypass attachment to a torus in detail. First, we introduce the Farey graph. We define the graph inductively. Let $\mathbb{D}$ be the Poincaré disk. Start with the top-most vertex labeled $0 = \frac{0}{1}$ and the bottom-most vertex labeled $\infty = \frac{1}{0}$ and connect them by a geodesic. Given two vertices in the right half plane which are already labeled $\frac{a}{b}$ and $\frac{c}{d}$, choose a vertex on $\partial\mathbb{D}$ in the middle of the vertices and label it as $\frac{a+c}{b+d}$. Then connect

it with the other two vertices by geodesics. For the left half plane, we treat ∞ as $-\infty = \frac{-1}{0}$. See Figure 2.5.

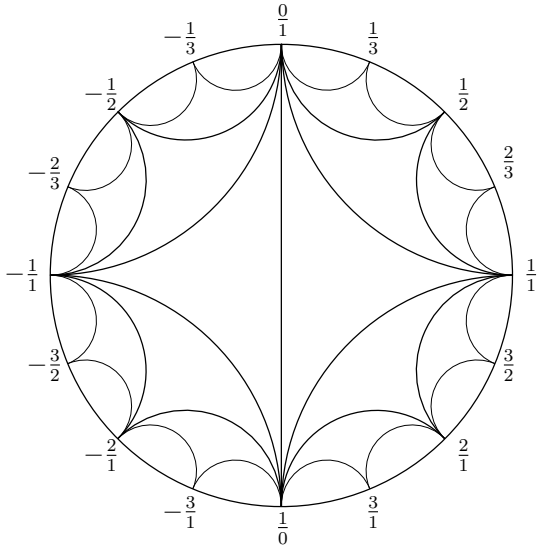

Figure 2.5: The Farey graph

Now consider a convex torus T^2 with two parallel dividing curves and a linear foliation. Choose a homology basis for T^2 as $(\binom{1}{0}, \binom{0}{1})$. Denote the slope of curves parallel to $\binom{p}{q}$ by $\frac{q}{p}$.

Theorem 2.1.6 (Honda [5])**.** *Let s and r be the dividing slope and ruling slope, respectively, of a convex torus T^2 with two dividing curves. After a bypass attachment to the front of T^2 along a ruling curve, we obtain a new convex torus with two dividing curves with slope s', where s' is the vertex on the Farey graph clockwise of s and counter-clockwise of r. In addition, s' is closest to r with an edge to s.*

Remark 2.1.7. If a bypass lies on the back of T^2, then Theorem 2.1.6 will hold after reversing the word "clockwise" and "counter-clockwise". Notice that here we use the *topologist's convention* for the slope of homologically non-trivial curves on $\partial(S^1 \times D^2)$. That is, $\binom{1}{0}$ is the longitudinal direction and $\binom{0}{1}$ is the meridional direction.

All of the results above are only useful when we can find a bypass. Fortunately, there are several ways to find a bypass.

Theorem 2.1.8 (Imbalance principle: Honda [5]). *Let Σ and $A = S^1 \times [0,1]$ be convex surfaces with Legendrian boundary. Suppose $\Sigma \cap A = S^1 \times \{0\}$ and $tw(S^1 \times \{0\}) < tw(S^1 \times \{1\}) \leqslant 0$. Then there is a bypass on Σ along $S^1 \times \{0\}$.*

Theorem 2.1.9 (Honda [5]). *Let Σ be a convex surface and D be a convex disk with a Legendrian boundary. Suppose $\Sigma \cap D = \partial D$. If $tb(\partial D) < -1$ then there is a bypass on Σ along ∂D.*

2.2 Basic slices and solid tori

Let $B := T^2 \times I$. A tight contact structure ξ on $T^2 \times I$ is called a *basic slice* if (1) $\partial B = T_0 \cup T_1$ is two standard convex tori with dividing slopes s_0 and s_1 respectively. (2) s_0 and s_1 are connected by an edge in the Farey graph. (3) the slope of the dividing curves on any convex torus T parallel to the boundary is between s_0 and s_1. This condition is called *minimal twisting*.

Theorem 2.2.1 (Honda [5]). *There are exactly two basic slices up to isotopy with a given boundary condition. These two tight contact structures are distinguished by their relative Euler class. They are called positive and negative basic slices and denoted by $B^+(s_0, s_1)$ and $B^-(s_0, s_1)$ respectively.*

Next, consider a solid torus $S^1 \times D^2$. Recall that $\binom{1}{0}$ be a longitudinal direction by a chosen framing and $\binom{0}{1}$ be a meridional direction. Suppose the boundary of $S^1 \times D^2$ is convex with two dividing curves. Kanda showed that there exists unique tight contact structures on this $S^1 \times D^2$ if the dividing slope is an integer, and Giroux and Honda completed the classification for general dividing slopes.

Theorem 2.2.2 (Kanda [10]). *Suppose the dividing curves are parallel to $\binom{1}{n}$. Then there exists a unique tight contact structure on $S^1 \times D^2$.*

Theorem 2.2.3 (Giroux [4], Honda [5]). *Let p, q be relatively prime integers. Suppose the dividing curves are parallel to $(\frac{q}{p})$, $q > -p \geqslant 1$. Then, the number of tight contact structures on $S^1 \times D^2$ up to isotopy is following:*

$$\pi_0(S^1 \times D^2, \Gamma) = |(r_0 + 1) \dots (r_{k-1} + 1) r_k|,$$

where

$$\frac{q}{p} = r_0 - \cfrac{1}{r_1 - \frac{1}{r_2 \dots - \frac{1}{r_k}}}$$

with $r_i \leqslant -2$.

If the slope $s = (\frac{q}{p})$ does not satisfy the condition $q > -p \geqslant 1$, use a self-diffeomorphism of $S^1 \times D^2$ which restricts to the Dehn twist on the boundary, whose matrix representation is $\left(\begin{smallmatrix} 1 & 0 \\ m & 1 \end{smallmatrix}\right)$, to change the framing and get a desired slope.

2.3 Contact surgery and Heegaard Floer homology

Consider a Legendrian knot L in (M, ξ). Let N be a standard neighborhood of L. *Contact $(\frac{p}{q})$-surgery* on L is defined as following: Let (λ, μ) be a contact framing and meridian for L, respectively. $M_{(p/q)}(L)$ is obtained by cutting N from M and re-gluing it via a diffeomorphism of ∂N sending μ to $p\mu + q\lambda$. Then, extend the contact structure $(M \backslash N, \xi)$ to the entire $M_{(p/q)}(L)$ so that it is tight on N.

In general, the number of possible extensions is not unique. This depends on how many contact structures exist on N with a given boundary condition. If we only focus on the tight contact structures on N, Theorem 2.2.3 gives the answer. Therefore, we obtain the following theorem.

Theorem 2.3.1 (Ding and Geiges [26]). *Let L be a Legendrian knot in (M, ξ) and p, q be relatively prime integers. Suppose $\frac{p}{q} < 0$. The number of contact structures (not necessarily*

non-isotopic) induced by contact $(\frac{p}{q})$-surgery on L is

$$|(r_0+1)\cdots(r_n+1)|$$

where

$$\frac{p}{q} = r_0 + 1 - \frac{1}{r_1 - \frac{1}{r_2 \cdots - \frac{1}{r_n}}}$$

with $r_i \leqslant -2$.

If p, q does not satisfy the condition $\frac{p}{q} < 0$, use $\frac{p}{q-kp}$ instead where k is the smallest positive integer such that $q - kp < 0$.

In [27], Ding, Geiges and Stipsicz exhibited an algorithm that converts any contact surgery diagram into a (± 1)-surgery diagram.

- contact $(\frac{p}{q})$-surgery with $\frac{p}{q} < 0$:
  1. Stabilize L $|r_0 + 2|$ times. Let this be L_0.
  2. For $n = 1, \ldots, n$, let L_i be the Legendrian push-off of L_{i-1} and stabilize it $|r_i + 2|$ times.
  3. Then a contact $(\frac{p}{q})$-surgery on L corresponds to a contact (-1)-surgeries on a link $(L_0, \ldots, L_n)$.
- contact $(\frac{p}{q})$-surgery with $\frac{p}{q} > 0$:
  1. Choose a positive integer k such that $q - kp < 0$. Let $r' = \frac{p}{q-kp}$.
  2. Let $L_1, \ldots, L_k$ be k successive Legendrian push-offs of L.
  3. Then a contact $(\frac{p}{q})$-surgery on L corresponds to $(+1)$-surgeries on $L, L_1, \ldots, L_{k-1}$ and a contact (r')-surgery on L_k.

Ozsváth and Szabó defined the Heegaard Floer homology $\widehat{HF}(M)$ in [28, 29], which is an invariant of a 3-manifold M. They also defined the Heegaard Floer contact invariant $c(\xi)$ of (M, ξ) in [30]. This invariant has the following properties.

Theorem 2.3.2 (Ozsváth and Szabó [30]). *The Heegaard Floer contact invariant $c(\xi)$ of (M, ξ) satisfies the following properties.*

- *If (M, ξ) is overtwisted, then $c(\xi) = 0$.*
- *If (M, ξ) is strongly fillable, then $c(\xi) \neq 0$.*

Recall that if (M, ξ) has a non-vanishing contact invariant $c(\xi)$, then contact surgery with a negative coefficient carries a non-vanishing contact invariant. For right-handed trefoil with the maximum Thurston-Bennequin number, positive contact surgery possesses a similar property.

Theorem 2.3.3 (Lisca and Stipsicz [31]). *Let L be a Legendrian right-handed trefoil in (S^3, ξ_{std}) with $tb(L) = 1$. For any $r \in \mathbb{Q}\backslash\{0\}$, contact r-surgery on L carries a non-vanishing contact invariant.*

2.4 Spin^c structure

Two non-vanishing vector fields v_0 and v_1 in a 3-manifold M are called *homologous* if they are homotopic through non-vanishing vector fields in $M\backslash D^3$. An equivalence class of homologous vector fields in M is called a spin^c structure on M. We denote the set of spin^c structures on M by $\mathrm{Spin}^c(M)$.

Consider a contact 3-manifold (M, ξ). Recall that any oriented 2-plane field on M naturally induces a spin^c structure by taking its oriented normal vector field. Thus, ξ induced a spin^c structure $\mathfrak{t}_\xi$. Moreover, it has the well-defined first Chern class $c_1(\mathfrak{t}_\xi)$.

Suppose (M, ξ) is obtained from (S^3, ξ_{std}) by a contact (± 1)-surgery on a Legendrian link. Since the smooth surgery coefficients are also integers, we can think the surgery diagram as a Kirby diagram and obtain a 4-manifold X. The contact structure ξ induces an almost complex structure J on ∂X and J extends to a complement of a 4-ball in $\mathrm{int}(X)$. Then there is the characteristic cohomology class $c \in H^2(X; \mathbb{Z})$, whose restriction to ∂X is $c_1(\mathfrak{t}_\xi)$. The following theorem had been first proved by Gompf in [32] for (-1)-contact

surgery diagrams and it was extended to contact (± 1)-surgery diagrams by Ding, Geiges and Stipsicz in [27].

Theorem 2.4.1 (Ding, Geiges and Stipsicz [27])**.** *Suppose X is a 4-manifold obtained from (± 1)-contact surgery diagram on a Legendrian link $\bigcup L_i$ in S^3 and ξ is a contact structure on ∂X induced by the contact surgery diagram. Denote the normal curves of the surgery knots by μ_i. Let c be its characteristic cohomology class. Then the following holds.*

$$\mathrm{PD}\left(c|_{\partial X}\right) = PD(c_1(\mathfrak{t}_\xi)) = \sum_{i=1}^{n} rot(L_i)[\mu_i]$$

.

CHAPTER 3

CONSTRUCTING CONTACT STRUCTURES VIA SURGERY

In this chapter, we will construct seven contact structures on the Weeks manifold via contact surgery and use contact classes in Heegaard Floer homology to show that they are tight. Then we will show these contact structures are pairwise non-isotopic. Consider the surgery diagram for the Weeks manifold W shown in Figure 1.1. After a left-handed Rolfsen twist on one link component K_2, the other component K_1 becomes a right-handed trefoil in S^3 as shown in Figure 3.1. After performing a sequence of blow-up operations, we obtain the surgery diagram shown in Figure 3.2. Realizing the link in Figure 3.2 as a Legendrian link, we obtain a contact surgery diagram shown in Figure 3.3. We apply the algorithm in section 2.3 to turn the diagram into (± 1)-contact surgery diagram and determine the number of contact structures (not necessarily different) induced by the diagram:

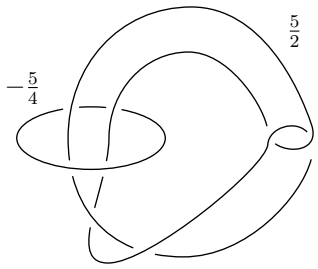

Figure 3.1: The result of left-handed Rolfsen twist on K_1

1. Take a Legendrian push-off of the Legendrian right-handed trefoil in Figure 3.3 and stabilize it twice. Perform contact $(+1)$-surgery on the original knot and (-1)-surgery on the push-off.

2. Perform (-1)-contact surgery on the other Legendrian unknots.

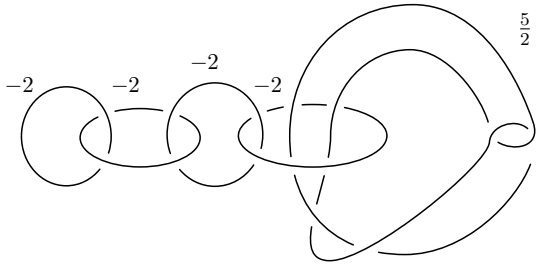

Figure 3.2: The result of blow-ups

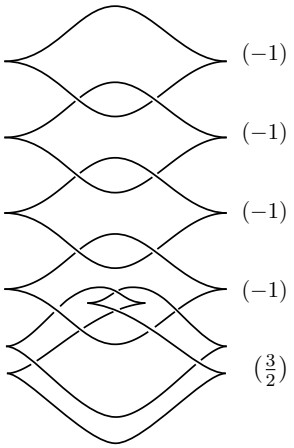

Figure 3.3: Legendrian realization of the link in Figure 3.2

Since there are three different Legendrian representatives of a twice stabilized Legendrian knot, the contact surgery diagram in Figure 3.3 induces three contact structures.

Since the Whitehead link is symmetric, we can switch the surgery coefficients of the link components K_1 and K_2. See the first drawing in Figure 3.4. Perform a left-handed Rolfsen twist on K_2, followed by a blow-up. We then obtain a surgery diagram with integer coefficients as shown in the bottom drawing of Figure 3.4. Realizing the link in the bottom drawing of Figure 3.4 as a Legendrian link, we obtain a contact surgery diagram shown in Figure 3.5. Again, we apply the algorithm in section 2.3 to turn the diagram into a (± 1)-contact surgery diagram:

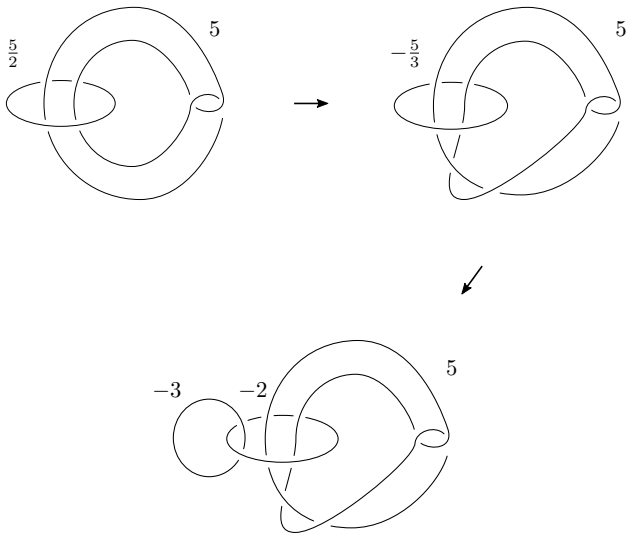

Figure 3.4: Another surgery diagram for the Weeks manifold.

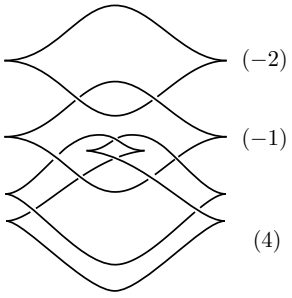

Figure 3.5: Legendrian realization of the third link in Figure 3.4.

1. Stabilize the Legendrian unknot in Figure 3.5 with contact surgery coefficient (-2) once and perform contact (-1)-surgery on it.

2. Take a Legendrian push-off of the Legendrian trefoil and stabilize it once. Then push off the result twice. Perform contact $(+1)$-surgery on the original knot and (-1)-surgeries on the push-offs.

3. Perform (-1)-contact surgery on the Legendrian unknot with contact surgery coefficient (-1).

Since there exist two different Legendrian representatives for a once stabilized Legendrian knot, the contact surgery diagram in Figure 3.5 induces four contact structures. Thus we obtain seven contact structures in total. Since both contact surgery diagrams consist of a positive contact surgery on the Legendrian right-handed trefoil with $\mathrm{tb} = 1$, followed by negative contact surgeries on the the other Legendrian knots, the Heegaard Floer contact class induced by the surgery diagrams are non-vanishing by Theorem 2.3.3. Hence all contact structures induced by Figure 3.3 and Figure 3.5 are tight. We now show that these contact structures are pairwise non-isotopic.

Proposition 3.0.1. *Each contact structure obtained from the contact surgery diagrams Figure 3.3 and Figure 3.5 induces distinct spin^c structures.*

Proof. It is enough to show that each contact structure has different first Chern classes. To this end, fix one contact structure first. In other words, fix the choice of stabilizations. Now according to Theorem 2.4.1, we can easily compute the Poincaré dual of the first Chern class of the contact structure. First, we consider the contact structures obtained from the surgery diagram in Figure 3.3. Recall that we took a push-off the trefoil in Figure 3.3 to turn the diagram into a (± 1)-contact surgery diagram. If we slide the push-off over the original trefoil, then we obtain the surgery diagram shown in the first drawing of Figure 3.6. Let the meridians of each surgery component of Figure 3.6 be $\eta_1, ..., \eta_6$ from left to right. Then the first homology of the Weeks manifold can be presented as

$$H_1(W;\mathbb{Z}) = \langle \eta_1, ..., \eta_6 \mid -2\eta_1 + \eta_2 = 0, \eta_1 - 2\eta_2 + \eta_3 = 0, \eta_2 - 2\eta_3 + \eta_4 = 0,$$
$$\eta_3 - 2\eta_4 = 0, 2\eta_5 + \eta_6 = 0, \eta_5 - 2\eta_6 = 0\rangle$$

and the Poincaré dual of the first Chern class of the contact structure can be $0\eta_1 + ... + 0\eta_5 \pm 2\eta_6$ or $0\eta_1 + ... + 0\eta_6$. Now we return back to the surgery diagram in Figure 1.1 by following Figure 3.6. Since the blowing up/down operations and Rolfsen twists induce a canonical self-diffeomorphism, we can keep track of the homology class under the diffeomorphisms. Let μ_1 and μ_2 be meridians of K_1 and K_2 respectively. Then the homology of the Weeks manifold is presented as

$$H_1(W;\mathbb{Z}) = \langle \mu_1, \mu_2 \mid 5\mu_1 = 5\mu_2 = 0\rangle,$$

and the Poincaré dual of the first Chern class is $\pm 4\mu_1 + 0\mu_2$ or $0\mu_1 + 0\mu_2$.

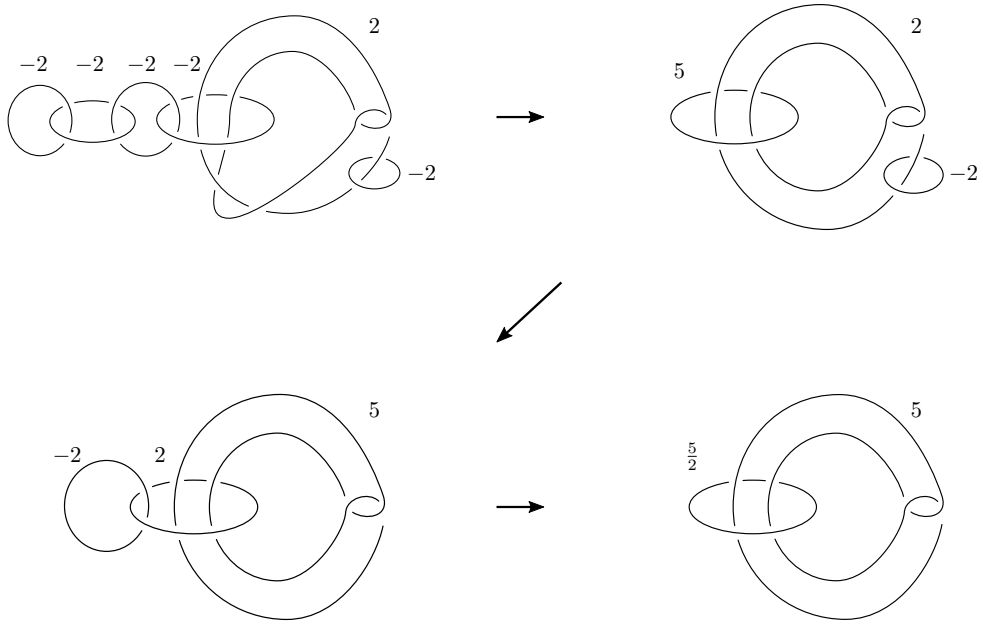

Figure 3.6: Returning back to the Whitehead link

Now consider the contact structures from Figure 3.5. Again, recall that we took the push-offs of the trefoil in Figure 3.5 to turn the surgery diagram into the (± 1)-contact surgery diagram. Slide the push-offs over the original trefoil and blow-down them. Then we obtain the surgery diagram shown in the last drawing of Figure 3.4. By performing a single blowing-down and Rolfsen twist, we obtain the surgery diagram in Figure 1.1. As above, by keeping track of the Poincaré dual of the first Chern class, we obtain $c = \pm 2\mu_1 \pm 3\mu_2$ or $c = \pm 2\mu_1 \mp 3\mu_2$.

Therefore, each contact structure induces different spin^c structures. Hence they are pairwise non-isotopic. □

Remark 3.0.2. In [31], Lisca and Stipsicz showed that a contact surgery on the Legendrian right-handed trefoil with $tb = 1$ in (S^3, ξ_{std}) preserves Stein fillability if the smooth surgery coefficient is greater than or equal to 4. Therefore, four contact structures on the Weeks manifold induced by Figure 3.3 are Stein fillable.

CHAPTER 4

AN UPPER BOUND ON TIGHT CONTACT STRUCTURES

In this section, we will find an upper bound of tight contact structures on the Weeks manifold W. We begin by decomposing the Weeks manifold into two simpler pieces.

4.1 A Rational open book decomposition

Consider the surgery diagram for the Weeks manifold W as shown in Figure 1.1. If we perform the surgery only on K_2, then the result will be $L(-5,1)$. Moreover, K_1 is a fibered knot in $L(-5,1)$ with a genus one fiber and the monodromy is given by

$$\psi = \begin{pmatrix} -3 & 1 \\ -1 & 0 \end{pmatrix}$$

which is the identity near the boundary. See [20, 33, 34] for more details on the fibration. Also note that ψ is an Anosov map. Let N be a small tubular neighborhood of K_1 and $M := L(-5,1)\backslash N$. Then $M = (\Sigma \times I)/\sim$, where $\Sigma = T^2\backslash D^2$ and $(x,1) \sim (\psi(x),0)$. We can obtain the Weeks manifold W by re-gluing N by a diffeomorphism $\phi : \partial N \to -\partial M$ given by

$$\phi = \begin{pmatrix} 1 & 2 \\ 2 & 5 \end{pmatrix}$$

For ∂N, here we set $\left(\begin{smallmatrix}1\\0\end{smallmatrix}\right)$ as a longitudinal direction given by the product framing of N and $\left(\begin{smallmatrix}0\\1\end{smallmatrix}\right)$ as a meridional direction of N. For $-\partial M$, We set $\left(\begin{smallmatrix}1\\0\end{smallmatrix}\right)$ as the direction given by $\partial\Sigma$ and $\left(\begin{smallmatrix}0\\1\end{smallmatrix}\right)$ as the direction given by $\{p\} \times I/\sim$, where $p \in \partial M$. The last direction is well-defined since ψ is the identity near $\partial\Sigma$.

Remark 4.1.1. In [34], Morimoto used a different gluing convention. That is, $M = (\Sigma \times$

$I)/\sim$ where $(x,0)\sim(\psi'(x),1)$. Thus the monodromy in [34] should be also different: $\psi'=\left(\begin{smallmatrix}-3 & -1\\ 1 & 0\end{smallmatrix}\right)$.

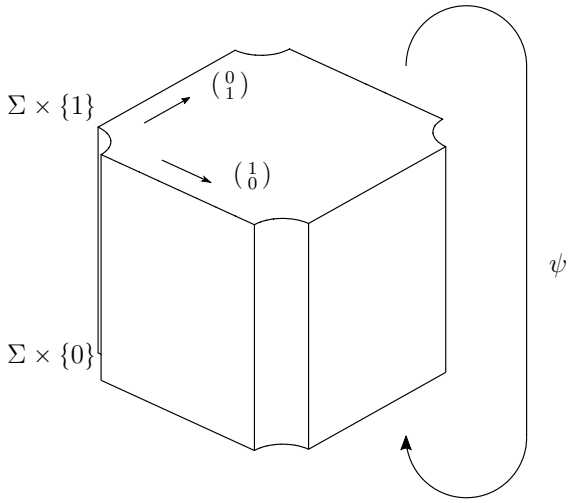

Figure 4.1: The bundle structure of $M=S^3\backslash N$. Opposite rectangles are identified. The top and bottom are glued by ψ.

Here, we will use the topologist's slope convention for N and ∂M. Recall that when we attach a bypass to N from the front, the slope changes in a clockwise direction on the Farey graph.

Consider the Weeks manifold (W,ξ) equipped with a contact structure ξ. Let L be a Legendrian knot in N isotopic to the core of N, which is the surgery dual knot of K_1. Now we can assume that N is a standard neighborhood of L after a perturbation. We can also make the ruling curves parallel to $\binom{5}{-2}$. Since $\phi\binom{5}{-2}=\binom{1}{0}$, the ruling curves are parallel to $\binom{1}{0}$ on $-\partial M$, which is parallel to $\partial\Sigma$. Therefore, we can make $\partial\Sigma$ Legendrian and perturb Σ to be a convex surface by Theorem 2.1.2.

From now on, when we say *the twisting number of* L, this means the twisting number of L with respect to the product framing on N.

To find the upper bound of the number of tight contact structures on W, we use the following strategy: First, start with L having a large negative twisting number. Then increase the twisting number by attaching bypasses to the standard neighborhood of L. Repeat this

and maximize the twisting number. Call it $\bar{s}$. Then count the number of potentially tight contact structures in each piece when L has the maximal twisting number $\bar{s}$. Finally, show that contact structures should be overtwisted if the twisting number of L is bigger than $\bar{s}$.

As mentioned above, to increase the twisting number of L, we need to find a bypass that can be attached to N, the standard neighborhood of L. To find such bypasses, we will use the method introduced by Etnyre and Honda in [35]. In [35], Etnyre and Honda showed that there exists a unique tight contact structure up to contactomorphism in the complement of the standard neighborhood of the figure-eight knot with $tb = -3$ in (S^3, ξ_{std}), which is a once-punctured torus bundle over S^1 with an Anosov monodromy. We will slightly generalize their method for any Anosov monodromy and apply this to our case.

Here, we outline how we will find an upper bound of tight contact structures on the Weeks manifold W. First, we will show that if the twisting number of L is greater than or equal to 0, then the contact structure is overtwisted. We then show that if the twisting number of L is less than -1, L can be destabilized. If the twisting number of L is -1, then we will find bypasses for N to make the dividing slopes of ∂N and ∂M to be $\left(\begin{smallmatrix}1\\-1\end{smallmatrix}\right)$ and $\left(\begin{smallmatrix}-1\\-3\end{smallmatrix}\right)$, respectively. Finally, with this boundary condition, we can arrange the dividing set on Σ to be one of two configurations, and we will show that in one configuration there exist at most four tight contact structures and in the other configuration, there exist at most three tight contact structures.

We begin by normalizing the dividing set of Σ. As discussed above, we can assume Σ is convex. Let U be a vertical invariant neighborhood of Σ. Then $M \backslash U = \Sigma \times [0,1]$. Let $\Sigma_t := \Sigma \times \{t\}$ for $0 \leqslant t \leqslant 1$ and Γ_t be a dividing set for Σ_t. We denote dividing curves with boundary by dividing arcs. From now on, we will use the Legendrian realization principle (Theorem 2.1.4) implicitly. First, observe the following simple lemma.

Lemma 4.1.2 (Etnyre and Honda [35])**.** *There are at most three distinct isotopy classes of properly embedded disjoint arcs on Σ which are not boundary parallel. Moreover, if there are closed curves on Σ, then there is at most one isotopy class of arcs and it is parallel to*

the closed curves. □

Proposition 4.1.3 (Etnyre and Honda [35]). *Suppose* Γ *consists of properly embedded arcs* $\gamma_1, \ldots, \gamma_n$ *and closed curves* $c_1, \ldots, c_m$. *Then one of the following holds.*

I. There is one isotopy class of arcs: (a) n *is odd, m=1,* (b) $n = 0$, $m = 2$, (c) $\exists$ *a bypass along* $\partial\Sigma$.

II. There are two isotopy classes of arcs: (a) $n = 4$ *and each isotopy class has two arcs,* (b) $\exists$ *a bypass along* $\partial\Sigma$.

III. There are three isotopy classes of arcs: (a) n *is odd and one isotopy class contains only one arc,* (b) $\exists$ *a bypass along* $\partial\Sigma$.

This proposition is due to Etnyre and Honda [35] but we present a proof for completeness.

Proof. The basic strategy of the proof is finding a bypass on Σ to modify the dividing set Γ. We will use an annulus $c \times I \subset \Sigma \times I$ where c is a closed curve on Σ and apply Imbalance principle (Theorem 2.1.8) to find a bypass.

Case I: First, observe that $m + n$ must be even to divide Σ. Choose a closed Legendrian curve c on Σ_0 which is parallel to curves in Γ_0 so that c does not intersect Γ_0. Consider an annulus $A := c \times I$ in $\Sigma \times I$. Then the geometric intersection number $|c \times \{1\} \cap \Gamma_1| \geqslant m + n > 0$ since an Anosov map does not preserve isotopy classes of curves and $\Gamma_0 = \psi(\Gamma_1)$. Hence we can find a bypass along $c \times \{1\}$ by Imbalance principle (Theorem 2.1.8).

Let p, q, r be intersection points between Γ_1 and the bypass in a consecutive order. Suppose $n \geqslant 2, m \geqslant 2$. In this case, p, q, r always lie on distinct dividing curves. If p, q or q, r lie on c_i's, m is reduced by 2 after attaching the bypass. If p, q or q, r lie on γ_i's, we obtain a bypass along $\partial\Sigma$. Now suppose $n = 1$, $m \geqslant 3$. In this case, any bypasses reduce m by 2. If $n > 2, m = 0$, any bypasses give rise to a bypass along $\partial\Sigma$. Now consider the case $n = 2, m = 0$. If $|c \times \{1\} \cap \Gamma_1| = 2$, we obtain a degenerate bypass along $c \times \{1\}$.

After attaching this bypass, we obtain a bypass along $\partial\Sigma$. Suppose $|c \times \{1\} \cap \Gamma_1| > 2$. Attaching a bypass along $c \times \{1\}$ results in the change of the slope of curves in Γ_1 according to Theorem 2.1.6. Moreover, Theorem 2.1.6 implies that $|c \times \{1\} \cap \Gamma_1| \geqslant 2$, so we can find a bypass along $c \times \{1\}$ again. After a finite sequence of attaching bypasses along $c \times \{1\}$, the slope of curves in Γ_1 and the slope of c are connected by an edge on the Farey graph, which implies $|c \times \{1\} \cap \Gamma_1| = 2$. Therefore, we obtain a degenerate bypass, which gives rise to a bypass along $\partial\Sigma$. To summarize, we eventually arrive to (a) $n \geqslant 1$ and $m = 1$, (b) $n = 0$ and $m = 2$, or (c) $\exists$ a bypass along $\partial\Sigma$.

Case II: First, note that $m = 0$ by Lemma 4.1.2. Denote the two isotopy classes by v_1 and v_2 respectively, and let n_1, n_2 be the numbers of arcs in each isotopy class. Note that n_1 and n_2 both must be even to divide Σ. Since ψ is an Anosov monodromy, there are two eigendirections for ψ. They form an attractive fixed point and a repelling fixed point respectively on the Farey graph. Denote the attractive eigendirection for ψ by p. Suppose v_1 is closer to p than v_2 on the Farey graph. Then $\psi(v_1)$ is closer to p than v_1, which implies it is different from both v_1 and v_2. Choose a closed curve c which is parallel to $\psi(v_1)$ so that $|c \cap \Gamma_0| = n_2$. Take an annulus $c \times I$ in $\Sigma \times I$. Then the intersection number $|c \times \{1\} \cap \Gamma_1| = n_1 + n_2$. Hence by Imbalance principle, we can find a bypass along $c \times \{1\}$.

Suppose $n_1, n_2 > 2$. Then p, q, r lie on distinct dividing curves and p, q or q, r are on curves with a same isotopy class. After attaching the bypass, we obtain a bypass along $\partial\Sigma$. Next, suppose $n_1 = 2, n_2 > 2$ (or $n_1 > 2, n_2 = 2$). In this case, the only bypasses which do not give rise to a bypass along $\partial\Sigma$ is the bypasses which pass only two dividing curves parallel to v_1 and p, r lie on the same dividing curve. Attaching this bypass results in the change of the slope of v_1. If $c \times \{1\}$ intersects the dividing curves parallel to v_1 in more than two points, then we can find such bypass again. After a sequence of attaching the bypasses, $c \times \{1\}$ intersects the dividing curves parallel to v_1 in only two points by Theorem 2.1.6. Then there cannot exist a bypass which does not produce a bypass along $\partial\Sigma$. The only remaining case is $n_1 = 2$ and $n_2 = 2$.

Case III: First, note that n must be odd to divide Σ. Denote the number of dividing curves in each isotopy class by n_1, n_2 and n_3. Use the same argument as in Case II to get a bypass on Σ_1. If $n_1, n_2, n_3 \geqslant 2$, then p, q, r lie on distinct dividing curves and p, q or q, r are on curves with a same isotopy class. Hence every possible bypass gives rise to a bypass along $\partial\Sigma$. Therefore, at least one isotopy class should contain only one curve. □

4.2 Twisting $\leqslant$ -1

In this section, we will show that if the twisting number of L is $\leqslant -1$, then we can always find a bypass along $\partial\Sigma$. First, suppose that the twisting number of L is -1. Then the dividing curves on ∂N are parallel to $\left(\begin{smallmatrix}1\\-1\end{smallmatrix}\right)$. Since $\phi\left(\begin{smallmatrix}1\\-1\end{smallmatrix}\right) = \left(\begin{smallmatrix}-1\\-3\end{smallmatrix}\right)$, the dividing curves on $-\partial M$ are parallel to $\left(\begin{smallmatrix}1\\3\end{smallmatrix}\right)$. Then the twisting number of $\partial\Sigma$ with respect to Σ is $tw(\partial\Sigma, \Sigma) = -|det\left(\begin{smallmatrix}1&1\\0&3\end{smallmatrix}\right)| = -3$. This implies that there are three dividing arcs on Σ by Theorem 2.1.3. Moreover, Lemma 4.1.2 and Proposition 4.1.3 implies that Γ is either Case I(a) with $n = 3, m = 1$ or Case III(a).

We now normalize Γ so that we can always assume Γ has one of two configurations. During the normalization, we can assume that we do not encounter a bypass along $\partial\Sigma$. If Γ is Case III(a) with three isotopy classes $v_1, v_2, v_3 \in \mathbb{Z}^2$, we will denote Γ by $\{v_1, v_2, v_3\}$. We also denote Γ by $\{s_1, s_2, s_3\}$ alternatively, where s_1, s_2, s_3 are the slopes of v_1, v_2, v_3 respectively. If Γ is Case I(a) with an isotopy class v, we will denote it by $\{v\}$ or $\{s\}$, where s is the slope of v.

Proposition 4.2.1. *There is an isotopic copy of* Σ *with a dividing set* $\Gamma = \{-\infty, -1, 0\}$ *or* $\{0, 1, \infty\}$

Suppose $\Gamma_1 = \{v_1, v_2, v_3\}$. Note that one isotopy class is the sum of the other two isotopy classes, so we can assume $v_2 = v_1 + v_3$ and $\{v_1, v_3\}$ are a basis for $\mathbb{Z}^2$. Hence $\{v_1, v_2, v_3\}$ form an ideal geodesic triangle on the Farey graph. We will find a bypass on Σ_1 and investigate the effect of the bypass attachment. After a sequence of bypass attachments, we arrive to either $\{-\infty, -1, 0\}$ or $\{0, 1, \infty\}$.

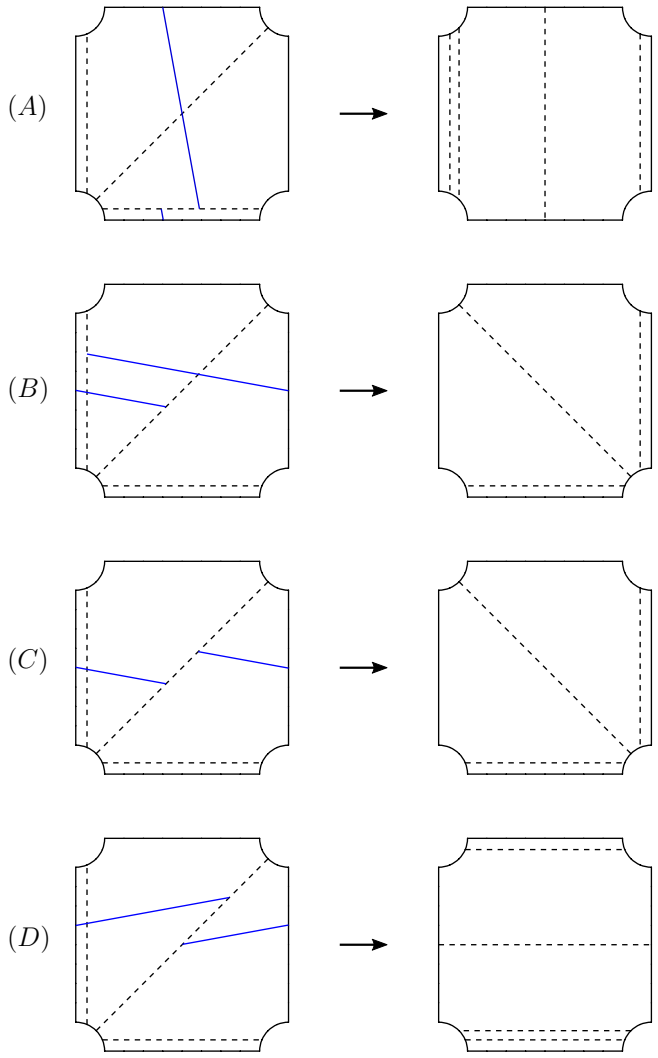

Figure 4.2: List of possible bypass attachments for Case III(a) with $n = 3$. The top and bottom are identified as are the left and right sides. The dashed lines represent dividing curves and the blue solid lines represent the attachment for the bypasses. The bypasses are attached from the back. For (A), (B) and (C), the slope of bypass attachment is less than 0. For (D), the slope of the bypass attachment is between 0 and 1.

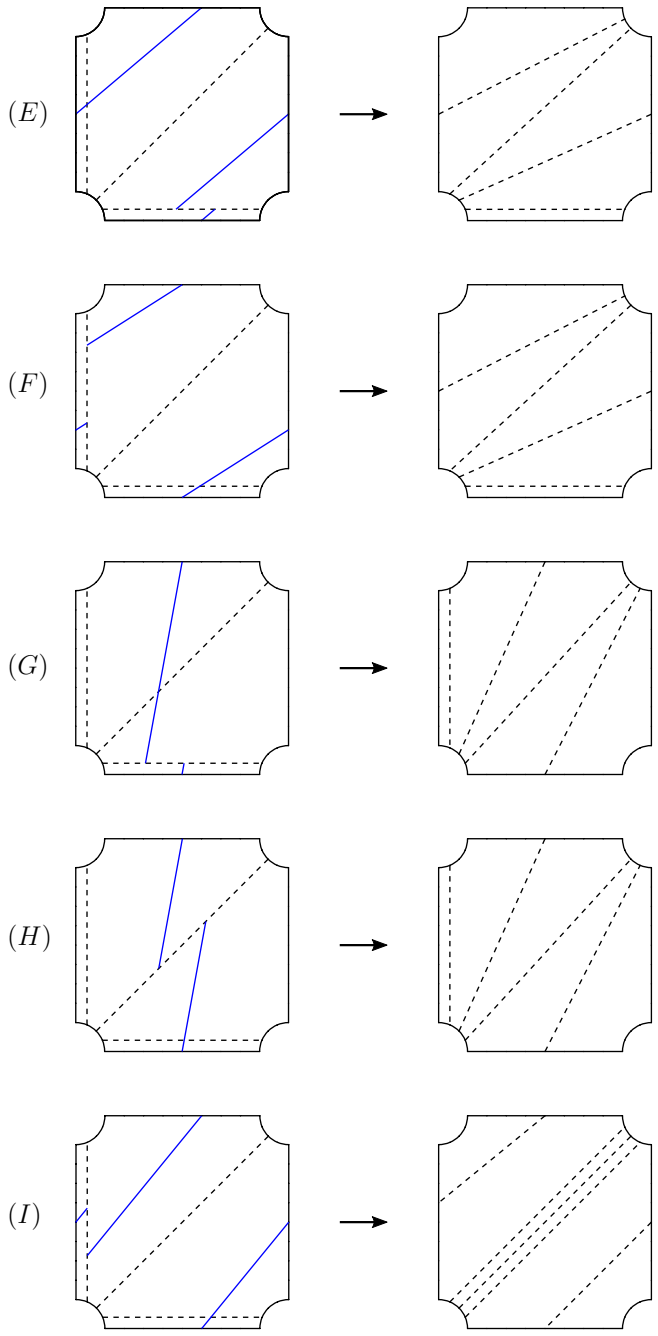

Figure 4.3: Continuation of list of possible bypass attachments for Case III(a) with $n = 3$. For (E) and (F), the slope of bypass attachment is between 0 and 1. For (G), (H) and (I), the slope of bypass attachment is between 1 and ∞.

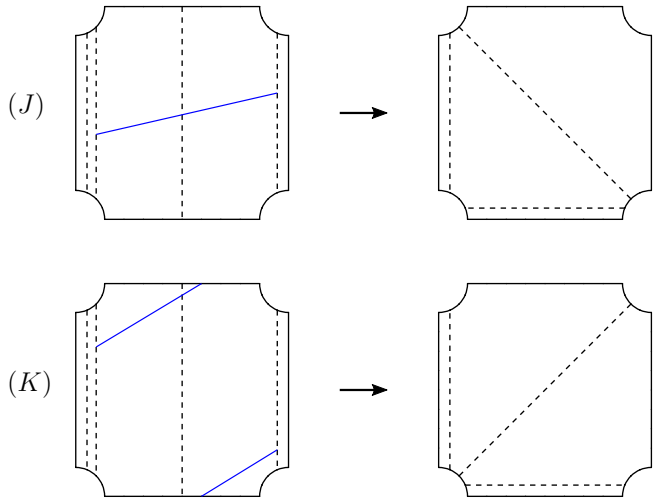

Figure 4.4: Two possible bypass attachment for Case I(a) with $n = 3, m = 1$.

Proof. First, we exhibit the complete list of possible bypass attachments on Σ_1 when Γ_1 is Case III(a). There are nine possible non-trivial bypass attachments which do not give rise to a bypass along $\partial\Sigma$. See Figure 4.2 and Figure 4.3 for the complete list. Note that the bypasses are attached on the back of Σ_1. See Figure 4.1. For $\Gamma_1 = \{v_1, v_2, v_3\}$, Take an orientation preserving diffeomorphism for T^2 which sends $\{v_1, v_2, v_3\} \mapsto \{0, 1, \infty\}$. Then find a corresponding bypass attachment from the list.

Let $p = \frac{3-\sqrt{5}}{2}$. Then $p, \frac{1}{p}$ are the eigendirections of ψ, where p is an attracting fixed point and $\frac{1}{p}$ is a repelling fixed point on the Farey graph. Consider an infinite cyclic covering space $\Sigma \times \mathbb{R}$ of $M = \Sigma \times I/\sim$. Since $\psi(\Sigma_1) = \Sigma_0$ and $\psi(\Gamma_1) = \Gamma_0$, the dividing set of $\Sigma \times \{k\}$ is $\psi^k(\Gamma_1)$ for any $k \in \mathbb{Z}$. Hence we can use $\psi^k(\Gamma_1)$ instead of Γ_1.

Suppose Γ_1 has a configuration of Case I(a). In this case, we can find a bypass on Σ_1 as in the proof of Proposition 4.1.3. Let p, q, r be intersection points between Γ_1 and the bypass in a consecutive order. If q is on a closed curve and p, r lie on arcs, the bypass attachment changes Γ_1 to become Case III(a). All other bypasses give rise to a bypass along $\partial\Sigma$. Hence we can assume Γ_1 has a configuration of Case III(a). Let $\Gamma_1 = \{v_1, v_2, v_3\}$ where $v_2 = v_1 + v_3$ and denote corresponding slopes by $\{s_1, s_2, s_3\}$ respectively. Since $\{v_1, v_2, v_3\}$ form an ideal geodesic triangle on the Farey graph as mentioned above, we act repeatedly

via ψ to make $s_1, s_2, s_3 \geqslant 0$ or $s_1, s_2, s_3 \leqslant 0$. To be precisely, we have following three cases:

1. $s_1 < s_2 < s_3 \leqslant 0 < p$
2. $0 \leqslant p < s_1 < s_2 < s_3 < \frac{1}{p}$
3. $0 \leqslant s_1 < p < s_2 < s_3 < \frac{1}{p}$ or $0 \leqslant s_1 < s_2 < p < s_3 < \frac{1}{p}$

(1) We will show that we can perform one of the following moves to the dividing set $\Gamma_1 = \{v_1, v_2, v_3\}$.

- $\{v_1, v_2, v_3\} \mapsto \{v_1 - v_3, v_1, v_3\}$: expanding the triangle to the counter-clockwise direction.
- $\{v_1, v_2, v_3\} \mapsto \{v_1, v_3, v_3 - v_1\}$: expanding the triangle to the clockwise direction.
- $\{v_1, v_2, v_3\} \mapsto \{v_3, v_4, v_5\}$: the biggest triangle starting from v_3 and v_4, v_5 are clockwise of v_3.
- $\{v_1, v_2, v_3\} \mapsto \{\binom{1}{0}\}$: type I(a) with slope 0.

After a finite sequence of the first three moves, we eventually arrive to $\{-\infty, -1, 0\}$. If we encounter the last move, act via ψ^{-1} and we obtain $\Gamma_1 = \{-\infty\}$. Now use an annulus $c \times I$ with slope 0 to find a bypass as in the proof of Proposition 4.1.3. This bypass attachment either gives rise to a bypass along $\partial\Sigma$ or changes the dividing set $\Gamma_1 = \{-\infty\}$ to $\{-\infty, -1, 0\}$. See Figure 4.4.

Now we will show that we can perform the above moves by attaching bypasses. First, note that $-\infty < s_3 \leqslant 0$ and $\psi(s_3) > 0$ because $\psi(-\infty) = 0$. Since $s_1, s_2 < 0$ and $\psi(s_3) > 0$, there are no connecting edges on the Farey graph between each s_1, s_2 and $\psi(s_3)$. Now take an annulus $c \times I$ with slope $\psi(s_3)$. Then the previous observation implies that $|\Gamma_1 \cap c \times \{1\}| > 2$ and $|\Gamma_0 \cap c \times \{0\}| = 2$. Therefore, we can find a bypass on

Σ_1 along $c \times \{1\}$ due to Imbalance principle (Theorem 2.1.8). Since $\psi(s_3)$ lies outside of the triangle formed by $\{v_1, v_2, v_3\}$ on the Farey graph, this bypass is of type A, B or C as shown in Figure 4.2. It can be explicitly checked by taking an orientation preserving diffeomorphism of T^2 which sends $\{v_1, v_2, v_3\}$ to $\{0, 1, \infty\}$. B and C change the triangle $\{v_1, v_2, v_3\}$ to either $\{v_1, v_3, v_3 - v_1\}$ or $\{v_1 - v_3, v_1, v_3\}$, which correspond to the first two moves in the above list. A changes $\{v_1, v_2, v_3\}$ to $\{v_3\}$. Now suppose v_3 is not $\left(\begin{smallmatrix}1\\0\end{smallmatrix}\right)$. Take an annulus $c \times I$ with slope $\psi(s_3)$ and find a bypass on Σ_1 as before. Let v be the isotopy class with the largest slope for which there exists an edge with v_3 on the Farey graph. Let $v' := v_3 - v$. Take an orientation preserving diffeomorphism of T^2 which sends $\{v', v_3, v\}$ to $\{1, -\infty, 0\}$. Since $\psi(s_3)$ is outside of the triangle $\{v', v_3, v\}$, it lies between $[0, 1]$ after acting via the diffeomorphism. Then there are only two possible bypass attachments which do not give rise to a bypass along $\partial\Sigma$. See Figure 4.4. J changes $\{v_3\}$ to $\{v_3, v_3 + v, v\}$ and K changes $\{v_3\}$ to $\{v', v_3, v\}$. The first move corresponds to a third move in the above list and the second move corresponds to a third move followed by a second move in the above list. Thus we can perform one of the moves in the list by attaching bypasses.

(2) After acting via ψ^k, we can assume $1 \leqslant s_1 < s_2 < s_3 \leqslant 2$. This is possible since $\psi(2) = 1$. Take an annulus with slope $\psi(s_1)$ and we obtain a bypass of type A, B or C as before. Using the same argument as in the case (1), we arrive to either $\Gamma_1 = \{2\}$ or $\Gamma_1 = \{1, \frac{3}{2}, 2\}$. In the first case, act via ψ^{-1} and we obtain $\Gamma_1 = \{1\}$. Take an annulus with slope $\psi(1) = \frac{1}{2}$ again to obtain a bypass. After the bypass attachment, we obtain $\{1\} \mapsto \{0, \frac{1}{2}, 1\}$, which will be dealt with in the case (3). Next assume $\Gamma_1 = \{1, \frac{3}{2}, 2\}$. Again, use an annulus with slope $\psi(1) = \frac{1}{2}$ to obtain a bypass. This bypass is of type B or C. Hence after attaching the bypass, we obtain $\{1, \frac{3}{2}, 2\} \mapsto \{1, 2, \infty\}$, which also will be dealt with in the case (3).

(3) Assume we can perform one of the following moves.

- $0 < s_1 < p < s_2 < s_3 < \infty$: $\{v_1, v_2, v_3\} \mapsto \{v_1, v_1 + v_2, v_2\}$.
- $0 < s_1 < s_2 < p < s_3 < \infty$: $\{v_1, v_2, v_3\} \mapsto \{v_2, v_2 + v_3, v_3\}$.

Consider a triangle $\{v_1, v_2, v_3\}$ in the Farey graph which straddle p. Then for some large integer k, a triangle $\{\psi^k(0), \psi^k(1), \psi^k(\infty)\}$ separates p and $\{v_1, v_2, v_3\}$. Because there are only finitely many triangles between $\{v_1, v_2, v_3\}$ and $\{\psi^k(0), \psi^k(1), \psi^k(\infty)\}$, we can obtain $\{\psi^k(0), \psi^k(1), \psi^k(\infty)\}$ after a finite sequence of the above moves. Acting via ψ^{-k}, we obtain $\{0, 1, \infty\}$.

Now we will show that we can go back to the case (1) or perform the moves in the above list by attaching bypasses. First, suppose $s_1 < p < s_2 < s_3$. Take an annulus with slope $\psi(s_2)$. Since p is an attractive fixed point, $s_1 < p < \psi(s_2) < s_2 < s_3$. Hence we can find a bypass on Σ_1 by Imbalance principle (Theorem 2.1.8) and the type of bypass is D, E or F. D gives $\{v_1, v_2, v_3\} \mapsto \{v_1\}$, which was already dealt with in Case (1). E and F give $\{v_1, v_2, v_3\} \mapsto \{v_1, v_1 + v_2, v_2\}$. Next, assume $s_1 < s_2 < p < s_3$. Use an annulus with slope $\psi(s_2)$ to find a bypass as above. The type of this bypass is G, H or I. I gives $\{v_1, v_2, v_3\} \mapsto \{v_2\}$ so we go back to the case (1). G and H give $\{v_1, v_2, v_3\} \mapsto \{v_2, v_2 + v_3, v_3\}$. □

In either case, we can always find a boundary parallel bypass.

Proposition 4.2.2. *If the twisting number of L is -1, there exists an isotopic copy of Σ containing a bypass along $\partial\Sigma$.*

Proof. The basic idea of the proof is same as before. We try to find a bypass on Σ to modify Γ. However, we will not use an annulus. Instead, we will use a disk to find a bypass. First, we round the edges of $\Sigma \times I$ to make its boundary convex. See Figure 4.5. Note that there is a holonomy on $\partial\Sigma \times I$. Then, we will look for a convex compressing disk D of $\Sigma \times I$ such that $tb(\partial D) < -1$. Then we can obtain a bypass along ∂D by Theorem 2.1.9.

By Proposition 4.2.1, we only need to consider the two following cases.

(1) $\Gamma_1 = \{0, 1, \infty\}$ and $\Gamma_0 = \{\frac{1}{3}, \frac{1}{2}, 0\}$: Note that the monodromy ψ is a *right-veering* diffeomorphism (cf. [36]) since it is a positive Dehn twist. Hence the dividing curves in Γ_0 are to the right of the curves in Γ_1. See Figure 4.6. The compressing disk D is shown as solid blue lines in Figure 4.6. The dividing curves on $\partial\Sigma \times I$ are shown in Figure 4.5.

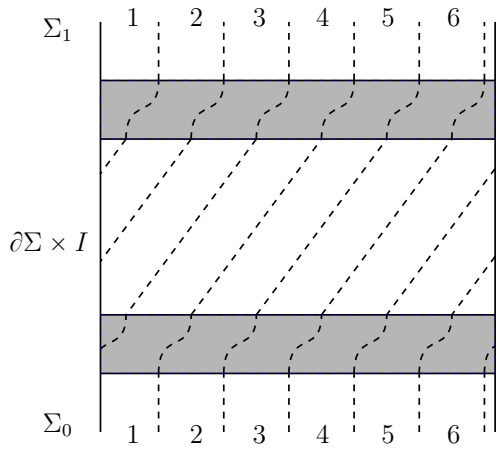

Figure 4.5: The left and right sides are identified. The dashed lines represent dividing curves. The top and bottom parts are neighborhoods of $\partial\Sigma_i$ in Σ_i and the middle part is the region $\partial\Sigma \times I$. The shaded regions are the result of edge-rounding. The dividing curves on Σ_i divide $\partial\Sigma_i$ into six intervals and they are labeled 1 to 6.

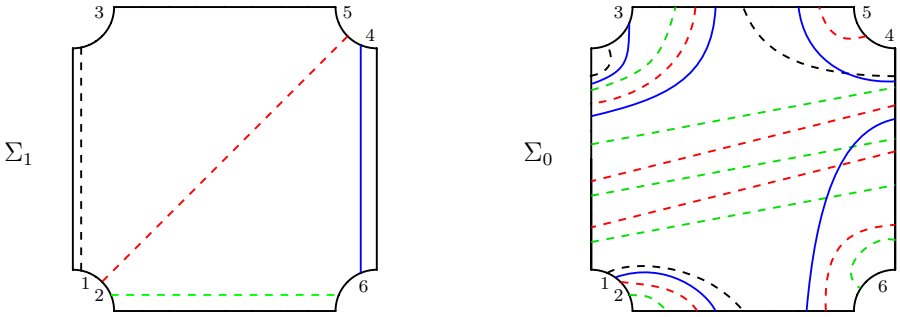

Figure 4.6: The dashed lines represent dividing curves on Σ_1 and Σ_0. The blue solid lines represent the intersection of the compressing disks D_1, D_2 with Σ_1 and Σ_0.

We can arrange D so that ∂D does not intersect any dividing curves on $\partial\Sigma \times I$. However, it changes the sides of the dividing curves where ∂D is on. Note that if ∂D is in the i-th interval of $\partial\Sigma \times \{1\}$, then ∂D is in the $(i-3)$-th interval (mod 6) of $\partial\Sigma \times \{0\}$. Thus $tb(\partial D) = -2$ and we can find a bypass along ∂D by Theorem 2.1.9. By Theorem 2.1.4, we can arrange the bypass to be on Σ_0. Note that this bypass lies on the front side of Σ_0. There are two possible bypasses on Σ_0 and they both give rise to a bypass along $\partial\Sigma$ after the bypass attachment.

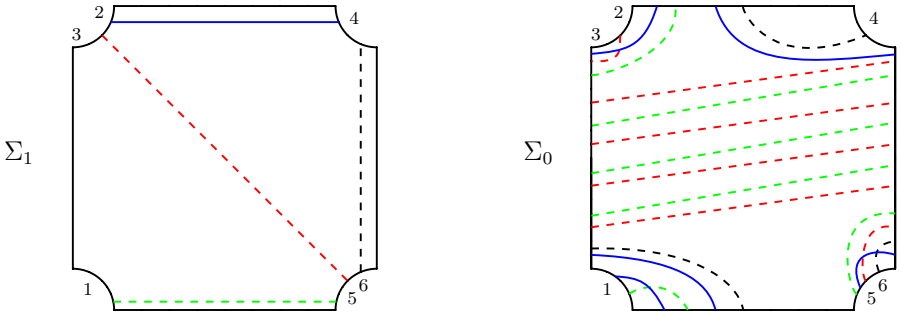

Figure 4.7: The dashed lines represent dividing curves on Σ_1 and Σ_0. The blue solid lines represent the intersection of the compressing disks D_1, D_2 with Σ_1 and Σ_0.

(2) $\Gamma_1 = \{-\infty, -1, 0\}$ and $\Gamma_0 = \{0, \frac{1}{4}, \frac{1}{3}\}$: The compressing disk D is shown as solid blue lines in Figure 4.7. As before, we can arrange D so that ∂D does not intersect any dividing curves on $\partial\Sigma \times I$. Thus $tb(\partial D) = -2$ and we can find a bypass on Σ_0 again. Note that there are two possible bypasses on Σ_0. A bypass which straddle a red dividing curve gives rise to a bypass along $\partial\Sigma$ and the other bypass which straddle a black dividing curve modifies Γ_0 and it becomes $\{0, \frac{1}{3}, \frac{1}{2}\}$. Acting via ψ^{-1}, we obtain $\Gamma_1 = \{0, 1, \infty\}$, which was already dealt with in (1). □

If the twisting number of L is less than -1, we can always find a bypass along $\partial\Sigma$. Hence the twisting number can be increased by Theorem 2.1.6. We will prove the following result in section 4.6

Proposition 4.2.3. *If the twisting number of L is less than -1, there exists an isotopic copy of Σ containing a bypass along $\partial\Sigma$.*

4.3 Finding tight contact structures

Suppose the twisting number of L is -1 again. In this case, there exists a bypass along $\partial\Sigma$ by Proposition 4.2.2. After attaching this bypass to N, the dividing slope becomes $\left(\begin{smallmatrix}2\\-1\end{smallmatrix}\right)$ by Theorem 2.1.6. Since $\phi\left(\begin{smallmatrix}2\\-1\end{smallmatrix}\right) = \left(\begin{smallmatrix}0\\-1\end{smallmatrix}\right)$, the dividing slope of $-\partial M$ is $\left(\begin{smallmatrix}0\\-1\end{smallmatrix}\right)$. The twisting number of $\partial\Sigma$ with respect to Σ is $-|det\left(\begin{smallmatrix}1&0\\0&-1\end{smallmatrix}\right)| = -1$. Hence there is only one dividing arc on Σ. By Proposition 4.1.3, we have Case I(a) with $n = 1, m = 1$ or there is a bypass along $\partial\Sigma$. In either case, we can find potentially tight contact structures on W. We start with Case I(a) first.

Proposition 4.3.1. *Suppose $\Gamma = \{v\}$ with one arc and one closed curve. Then there exists an isotopic copy of Σ such that $\Gamma = \{\infty\}$.*

Proof. Let s be the slope of v. Acting via ψ repeatedly, there are only two possibilities: (1) $s \leqslant 0 < p$, (2) $p < s < \frac{1}{p}$. Consider the first case. Suppose s is not already $-\infty$ or 0. Since $\psi(-\infty) = 0$, $s < 0$ and $\psi(s) > 0$. Take an annulus with slope $\psi(s)$ to obtain a bypass on Σ_1 as before. After attaching the bypass, the slope changes in a clockwise direction on the Farey graph by Theorem 2.1.6. After a sequence of the bypass attachments, we eventually arrive to $\Gamma_1 = \{0\}$. Acting via ψ^{-1}, we obtain $\Gamma_1 = \{\infty\}$. Next, suppose $p \leqslant s \leqslant \frac{1}{p}$. Acting via ψ repeatedly, we can further assume that $1 \leqslant s < 2$. Since $\psi(2) = 1$, $\psi(s) < 1$. Suppose s is not already 1. Take an annulus with slope $\psi(s)$ to obtain a bypass on Σ_1. This bypass modifies the slope s in a clockwise direction on the Farey graph, so we eventually arrive to $s = 2$. Acting via ψ^{-1}, we obtain $s = 1$. Take an annulus with the slope -1 to obtain a bypass on Σ_0. Note that this bypass is on the front of Σ_0. The bypass changes Γ_0 from $\{\frac{1}{2}\}$ to $\{0\}$. Hence Γ_1 becomes $\{\infty\}$. □

Proposition 4.3.2. *There exist two non-isotopic potentially tight contact structures on $\Sigma \times I$ where Γ_1 is Case I(a). In this case, there exist four potentially tight contact structures on W up to isotopy.*

Proof. Because $\Sigma \times I$ is a genus two handlebody, we will choose two convex compressing disks and cut the handlebody along the disks. The result manifold is a 3-ball and there exists unique tight contact structures on a 3-ball. Thus, the number of potentially tight contact structures on M is determined by the number of possible configurations of dividing curves on the disks and the signs of regions $\Sigma \backslash \Gamma$.

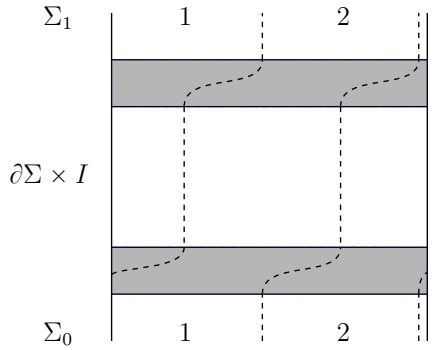

Figure 4.8: The left and right sides are identified. The dashed lines represent dividing curves. The top and bottom parts are neighborhoods of $\partial\Sigma_i$ in Σ_i and the middle part is the region $\partial\Sigma \times I$. The shaded regions are the result of edge-rounding. The dividing curves on Σ_i divide $\partial\Sigma_i$ into two intervals and they are labeled 1 and 2 respectively.

By Proposition 4.3.1, we can assume $\Gamma_1 = \{\infty\}$ and $\Gamma_0 = \{0\}$. Note that there can exist a boundary twisting on Σ, which is the result of Dehn twists along a boundary parallel closed curve. Arrange the boundary twisting to be near the boundary and cut M along a convex torus parallel to the boundary containing the boundary twisting. If the boundary slope of the convex torus is bigger than $-\infty$, we obtain a basic slice. Note that every holonomy in a basic slice is equivalent. If the boundary slope of the convex torus is ∞, glue $T^2 \times I$ layer to N. It does not change the boundary slope of N and remove the boundary twisting of Σ. Hence we can fix one configuration without a boundary twisting.

Now, round edges of $\Sigma \times I$ to make it have a convex boundary. See Figure 4.8. Then

choose two compressing disks D_1, D_2 as shown in Figure 4.9. Arrange the disks so that they do not intersect any dividing curves on $\partial\Sigma \times I$. Hence $tw(\partial D_i) = -1$ and there is a unique configuration of dividing curves for D_i. Now isotopy classes of contact structures on M are only determined by the signs of regions $\Sigma\backslash\Gamma$. Since we have two choices for the signs, there exist two potentially tight contact structures on M up to isotopy. Since there are two tight contact structures on the solid torus N with boundary slope $-\frac{1}{2}$ by Theorem 2.2.3, there exist four potentially tight contact structures on W up to isotopy. □

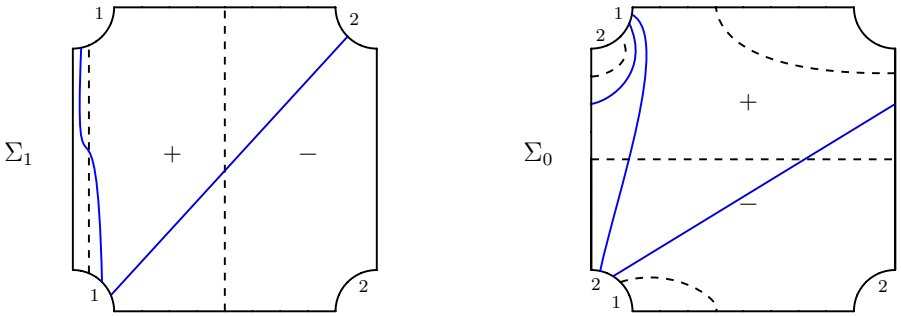

Figure 4.9: The dashed lines represent dividing curves on Σ_1 and Σ_0. The blue solid lines represent the intersection of the compressing disks with Σ_1 and Σ_0.

Now consider the bypass case. Observe that there are two types of closed curves on Σ: boundary parallel closed curves and essential(non-boundary parallel) closed curves. We begin by normalizing the dividing set.

Proposition 4.3.3. *Suppose Γ contains one boundary parallel arc and closed curves. Then, one of the following holds.*

IV. One boundary parallel arc and n closed boundary parallel curves.

V. One boundary parallel arc without closed curves.

Proof. Let m, n be the number of essential closed curves and closed boundary parallel curves in Γ respectively. First, assume $m > 2$. We can reduce m to 2 by the same argument as in Proposition 4.1.3 and make essential curves parallel to $\binom{0}{1}$ as in Proposition 4.3.2.

Cut $\Sigma \times I$ along the compressing disk as shown in Figure 4.10. Because ∂D has four more intersection points with Γ_1 than with Γ_0, we can always find a bypass on Σ_1. This bypass attachment reduces the number of dividing curves in Γ_1 by two. After a sequence of the bypass attachments, we eventually arrive in either Case I(a) with $n = 1$, Case IV or Case V': one boundary parallel arc with $n = 0, m = 2$. Suppose we have Case V'. Take a compressing disk D with slope 0 again. Then we can arrange D so that ∂D intersect Γ_1 four times and does not intersect Γ_0. Hence we can find a bypass on Σ_1 along ∂D. After attaching the bypass, we obtain Case V with $n = 0, m = 0$. □

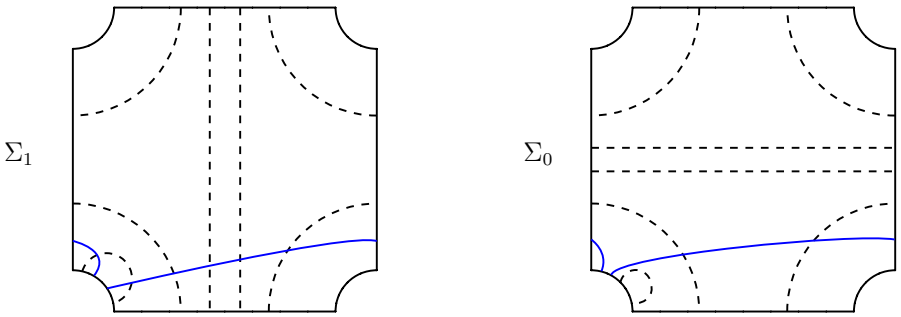

Figure 4.10: The dashed lines represent dividing curves on Σ_1 and Σ_0. The blue solid lines represent the intersection of the compressing disk with Σ_1 and Σ_0.

Let us consider Case IV. Let n be the number of boundary parallel closed curves in Γ. Take a compressing disk D as shown in Figure 4.11. Suppose there is a bypass on Σ_1. If $n \geqslant 2$, this bypass reduces the number of closed curves by 2. If $n = 1$, Γ becomes Case I(a). There is a unique configuration for D which does not contain a bypass on Σ_1. See Figure 4.12. This corresponds to the product contact structure on $\Sigma \times I$ since the other configurations contain non-trivial bypasses on Σ_1. We will show that in this case we obtain an overtwisted contact structure on W.

Proposition 4.3.4. *Consider a product contact structure on $\Sigma \times I$ for which Γ_1 is Case IV. This contact structure induces an overtwisted contact structure on W.*

Proof. Choose a point p on a closed dividing curve in Γ_1. Take an arc $p \times [0, 1]$. Then the arc is Legendrian and the contact planes do not twist along the arc with respect to the

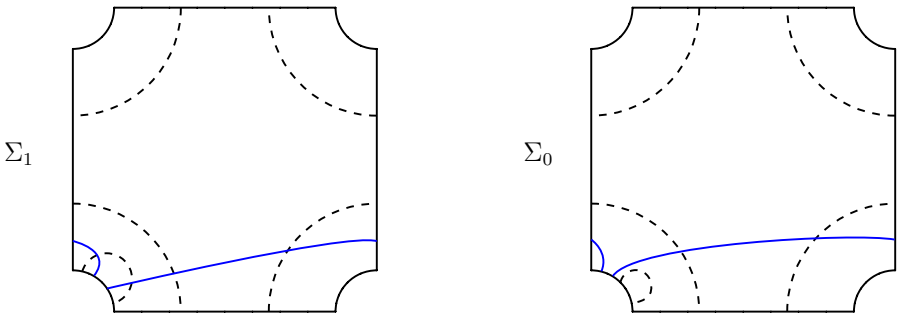

Figure 4.11: The dashed lines represent dividing curves on Σ_1 and Σ_0. The blue solid lines represent the intersection of the compressing disk with Σ_1 and Σ_0.

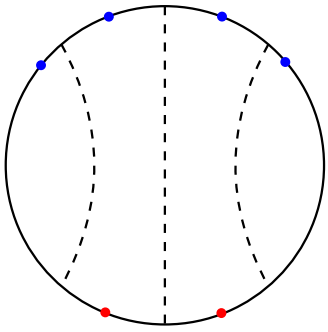

Figure 4.12: The dashed lines represent dividing curves on the compressing disk D. The blue dots represent the intersection points of D and Γ_1 and the red dots represent the intersection points of D and Γ_0.

product structure. Since ψ is an identity near $\partial\Sigma$, the arc $p \times [0,1]$ becomes a Legendrian closed curve in $M = \Sigma \times I/\sim$ and the contact planes do not twist along the curve with respect to the fibration structure. Hence we can find a convex torus parallel to $-\partial M$ whose dividing slope is ∞, which is parallel to S^1-direction. Between this torus and $-\partial M$, we can find another convex torus whose dividing slope is 0, which is parallel to $\partial\Sigma$ by Legendrian realization principle (Theorem 2.1.4). This implies that there is a non-minimal twisting $T^2 \times I$ layer in M and after gluing this to the solid tours N, the result contains a convex torus parallel to ∂N with dividing curves parallel to meridional direction. Hence the contact structure induces an overtwisted contact structure on W. □

Proposition 4.3.5. *There exist two non-isotopic potentially tight contact structures on $\Sigma \times I$ where Γ is Case V. In this case, there exist four potentially tight contact structures on W up to isotopy.*

Proof. The proof is basically same as the proof of Proposition 4.3.2. First round edges of $\Sigma \times I$ to make its boundary convex. Choose two convex compressing disks D_1, D_2 as shown in Figure 4.13. After cutting the handlebody along the disks, we obtain a 3-ball. There is only one configuration of dividing curves in each disk since $tb(\partial D_i) = -1$. Hence contact structures are determined by the sign of the regions $\Sigma \backslash \Gamma$ as before. Therefore there exist two potentially tight contact structures on $\Sigma \times I$ up to isotopy. Since the number of tight contact structures on the solid torus N with dividing slope $-\frac{1}{2}$ is two by Theorem 2.2.3, there exist four potentially tight contact structures on W. □

Remark 4.3.6. James Conway showed in [37] that potentially tight contact structures on $\Sigma \times I$ from Proposition 4.3.2 and Proposition 4.3.5 are actually tight and not contactomorphic.

To summarize, there exist eight non-isotopic potentially tight contact structures on W. We will improve the situation in the next section.

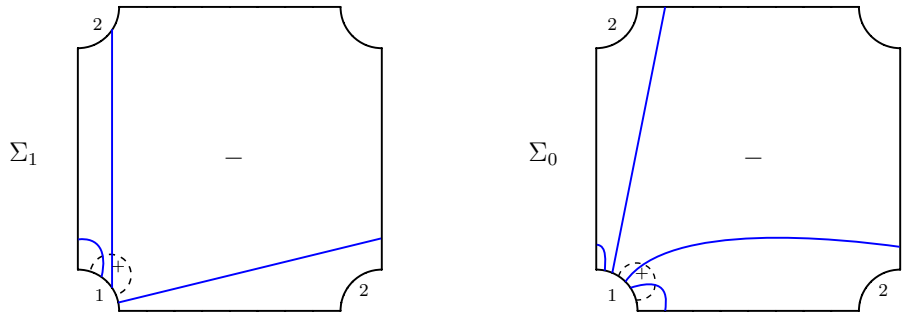

Figure 4.13: The dashed lines represent dividing curves on Σ_1 and Σ_0. The blue solid lines represent the intersection of the compressing disks with Σ_1 and Σ_0.

4.4 Bypass case

Consider a surgery diagram for W shown in Figure 3.1. Since this diagram is the result of a left-handed Rolfsen twist on K_2 of the diagram shown in Figure 1.1, it gives the same decomposition as before. Hence we can realize K_1 as a Legendrian knot with $tb = 1$ as shown in Figure 3.3. Thus, the dividing curves in $-\partial M$ is parallel to $\left(\begin{smallmatrix}1\\1\end{smallmatrix}\right)$. Since $\phi^{-1}\left(\begin{smallmatrix}1\\1\end{smallmatrix}\right) = \left(\begin{smallmatrix}3\\-1\end{smallmatrix}\right)$, the dividing slope of N is $-\frac{1}{3}$. Because the twisting number of $\partial\Sigma$ with respect to Σ is $-|det\left(\begin{smallmatrix}1&1\\0&1\end{smallmatrix}\right)| = -1$, the number of dividing arcs on Σ is 1. Therefore, we have Case I(a) with $n = 1, m = 1$ or there exists a bypass along $\partial\Sigma$.

Consider the bypass case first. After attaching the bypass to N, the dividing slope becomes $s = \left(\begin{smallmatrix}5\\-2\end{smallmatrix}\right)$ by Theorem 2.1.6. This implies that the bypass layer contains a convex torus parallel to ∂N with the dividing slope $\left(\begin{smallmatrix}0\\1\end{smallmatrix}\right)$ between $\left(\begin{smallmatrix}3\\-1\end{smallmatrix}\right)$ and $\left(\begin{smallmatrix}5\\-2\end{smallmatrix}\right)$. Since $\left(\begin{smallmatrix}0\\1\end{smallmatrix}\right)$ is the meridional slope, we obtain an overtwisted contact structure on W.

Now consider Case I(a) with $n = 1, m = 1$. We can normalize Γ_1 so that $\Gamma_1 = \{\left(\begin{smallmatrix}0\\1\end{smallmatrix}\right)\}$ by the same argument as in Proposition 4.3.1. Let $N(s)$ be the solid torus with the boundary dividing slope s. Now factor the solid torus $N(-\frac{1}{3})$ into $N(-1)$ and two basic slices $B(-1,-\frac{1}{2}), B(-\frac{1}{2},-\frac{1}{3})$. Note that $B(-1,-\frac{1}{2})$ and $B(-\frac{1}{2},-\frac{1}{3})$ are continued fraction blocks so we can shuffle the bypass layer. Especially, $B^+(-1,-\frac{1}{2}) \cup B^-(-\frac{1}{2},-\frac{1}{3}) = B^-(-1,-\frac{1}{2}) \cup B^+(-\frac{1}{2},-\frac{1}{3})$.

Let $M(s)$ be $\Sigma\times I/\sim$ with the boundary dividing slope s. Suppose $(M(1), \Gamma_1 = \{\left(\begin{smallmatrix}0\\1\end{smallmatrix}\right)\})$

admits more than one tight contact structure. Let $M_\xi := (M(1), \Gamma_1, \xi)$ and $M_{\xi'} := (M(1), \Gamma_1, \xi')$ be two tight contact structures on $(M(1), \Gamma_1)$. Now consider basic slices $B^{\pm}(-\frac{1}{2}, -\frac{1}{3})$. Here, slopes are measured with respect to the coordinate system of N. Since $\phi(-\frac{1}{2}) = \infty$ and $\phi(-\frac{1}{3}) = 1$, we can glue this basic slice to $M(1)$ and we arrive to $M(\infty)$ with a bypass along $\partial\Sigma$. See Figure 4.14. By Proposition 4.3.5, there exist exactly two potentially tight contact structures up to isotopy on $M(\infty)$ with a bypass along $\partial\Sigma$, and the isotopy classes are determined by the sign of a bypass. Denote them by $M(\infty)^{\pm}$ according to the sign of a bypass. Then, we obtain $M_\xi \cup B^{\pm}(-\frac{1}{2}, -\frac{1}{3}) = M(\infty)^{\pm} = M_{\xi'} \cup B^{\pm}(-\frac{1}{2}, -\frac{1}{3})$. No matter how many tight contact structures $(M(1), \Gamma_1)$ admits, we arrive to one of two tight contact structures on $M(\infty)$, which is only determined by the sign of the basic slice. Therefore, we can fix one tight contact structure on $(M(1), \Gamma_1 = \{\binom{0}{1}\})$.

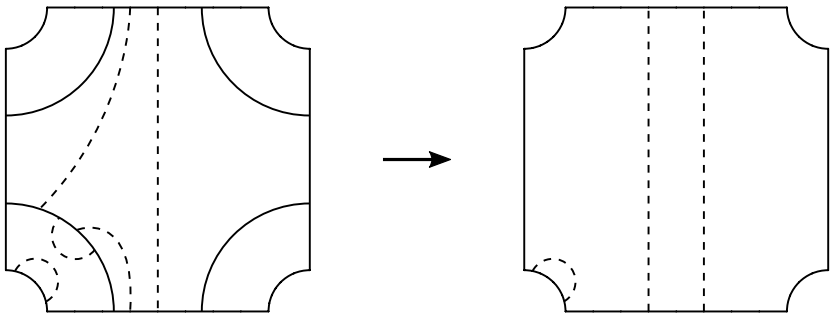

Figure 4.14: Gluing two tight contact structures.

Consider the situation of Proposition 4.3.5. We have two tight contact structures $M(\infty)^{\pm}$. We also have two tight contact structures on $N(-\frac{1}{2})$, which are determined by the sign of basic slice $N(-1, -\frac{1}{2})$. Denote them by $N(-\frac{1}{2})^{\pm}$. Hence four potentially tight contact structures on W can be expressed as following:

$$N(-\frac{1}{2})^{+} \cup M(\infty)^{+}$$

$$N(-\frac{1}{2})^{-} \cup M(\infty)^{+}$$

$$N(-\frac{1}{2})^{+} \cup M(\infty)^{-}$$

$$N(-\frac{1}{2})^- \cup M(\infty)^-$$

By the above discussion, we can decompose them further:

$$N(-1) \cup B^+(-1,-\frac{1}{2}) \cup B^+(-\frac{1}{2},-\frac{1}{3}) \cup M(1)$$

$$N(-1) \cup B^-(-1,-\frac{1}{2}) \cup B^+(-\frac{1}{2},-\frac{1}{3}) \cup M(1)$$

$$N(-1) \cup B^+(-1,-\frac{1}{2}) \cup B^-(-\frac{1}{2},-\frac{1}{3}) \cup M(1)$$

$$N(-1) \cup B^-(-1,-\frac{1}{2}) \cup B^-(-\frac{1}{2},-\frac{1}{3}) \cup M(1)$$

However, since $B(-1,-\frac{1}{2})$ and $B(-\frac{1}{2},-\frac{1}{3})$ are continuous fraction blocks, we can shuffle the bypass layers. Therefore, the second and third contact structures in the above list are isotopic, so there are only three potentially tight contact structures up to isotopy. Thus, we have proved the following proposition.

Proposition 4.4.1. *Suppose we have $(M(\infty),\Gamma)$ where Γ is Case V. In this case, there exist three potentially tight contact structures on W up to isotopy.* □

4.5 Twisting $\geqslant 0$

First, suppose the twisting number of L is bigger than 0. Stabilize L finitely many times to make the the twisting number 0. Therefore, we only need to consider the case that the twisting number is 0. In this case, the dividing slope of ∂N is $s = \left(\begin{smallmatrix}1\\0\end{smallmatrix}\right)$. Since $\phi\left(\begin{smallmatrix}1\\0\end{smallmatrix}\right) = \left(\begin{smallmatrix}1\\2\end{smallmatrix}\right)$, the dividing slope of $-\partial M$ is $\left(\begin{smallmatrix}1\\2\end{smallmatrix}\right)$. The twisting number of $\partial\Sigma$ with respect to Σ is $-|det\left(\begin{smallmatrix}1&1\\0&2\end{smallmatrix}\right)| = -2$. Thus, there are two dividing arcs on Σ and by Proposition 4.1.3, we can always find a bypass along $\partial\Sigma$. After attaching this bypass to N, the diving slope of ∂N becomes $\left(\begin{smallmatrix}2\\-1\end{smallmatrix}\right)$. This implies that we can find a convex torus parallel to ∂N with dividing slope $\left(\begin{smallmatrix}0\\1\end{smallmatrix}\right)$ between $\left(\begin{smallmatrix}1\\0\end{smallmatrix}\right)$ and $\left(\begin{smallmatrix}2\\-1\end{smallmatrix}\right)$. Because $\left(\begin{smallmatrix}0\\1\end{smallmatrix}\right)$ is the meridional slope of N, the contact structure on W is overtwisted.

Thus, there exists at most seven tight contact structures on W up to isotopy.

4.6 Thickening the solid torus

In this section, we will prove Proposition 4.2.3. Suppose the twisting number of L is $n < -1$. Then the dividing slope of ∂N is $\binom{1}{n}$. Since $\phi\binom{1}{n} = \binom{1+2n}{2+5n}$, the twisting number of $\partial\Sigma$ with respect to Σ is $-|det\left(\begin{smallmatrix} 1 & 1+2n \\ 0 & 2+5n \end{smallmatrix}\right)| = 2 + 5n \leqslant -8$. This implies there are at least eight dividing arcs on Σ. First, we will normalize Γ as in Proposition 4.2.1. Let $mult(s)$ be the number of dividing curves in the isotopy class with slope s.

Proposition 4.6.1. *There is an isotopic copy of Σ with a dividing set $\Gamma = \{\infty\}$, or $\Gamma = \{0, 1, \infty\}$ with $mult(0) = mult(\infty) = 1$ and $mult(1) = |4 + 5n|$.*

Proof. As discussed above, if $n < -1$, the number of dividing arcs on Σ is $-2-5n \geqslant 8$. In this case, Proposition 4.1.3 implies that Γ can be normalized so that we can assume either Case I(a) or Case III(a). Suppose we have Case I(a). Let $\Gamma_1 = \{s\}$. Then as in the proof of Proposition 4.2.1, choose an annulus with slope $\psi(s)$ to get a bypass on Σ_1. The only bypass which does not give rise to a bypass along $\partial\Sigma$ changes Γ to become Case III(a). See Figure 4.17. Hence we can assume Γ is Case III(a).

Figure 4.15 and Figure 4.16 show the all possible bypass attachments on Σ_1 which do not give rise to a bypass along $\partial\Sigma$ when Γ_1 is Case III(a). For $\Gamma_1 = \{v_1, v_2, v_3\}$, Take an orientation preserving diffeomorphism for T^2 which sends $\{v_1, v_2, v_3\} \mapsto \{0, 1, \infty\}$. Then find a corresponding bypass attachment from the list.

The basic idea is same as the proof of Proposition 4.2.1. We will use an annulus $c \times I \subset \Sigma \times I$ to find a bypass and modify Γ_1. Suppose $\Gamma_1 = \{v_1, v_2, v_3\}$ and corresponding slopes are $\{s_1, s_2, s_3\}$. If $mult(s) > 1$ for two isotopy classes, we have one of moves A, B or C in Figure 4.15. After a sequence of these moves, we can assume that two isotopy classes have $mult = 1$. Let $p, \frac{1}{p}$ be the eigendirections of ψ. After acting via ψ^k, we have three possibilities:

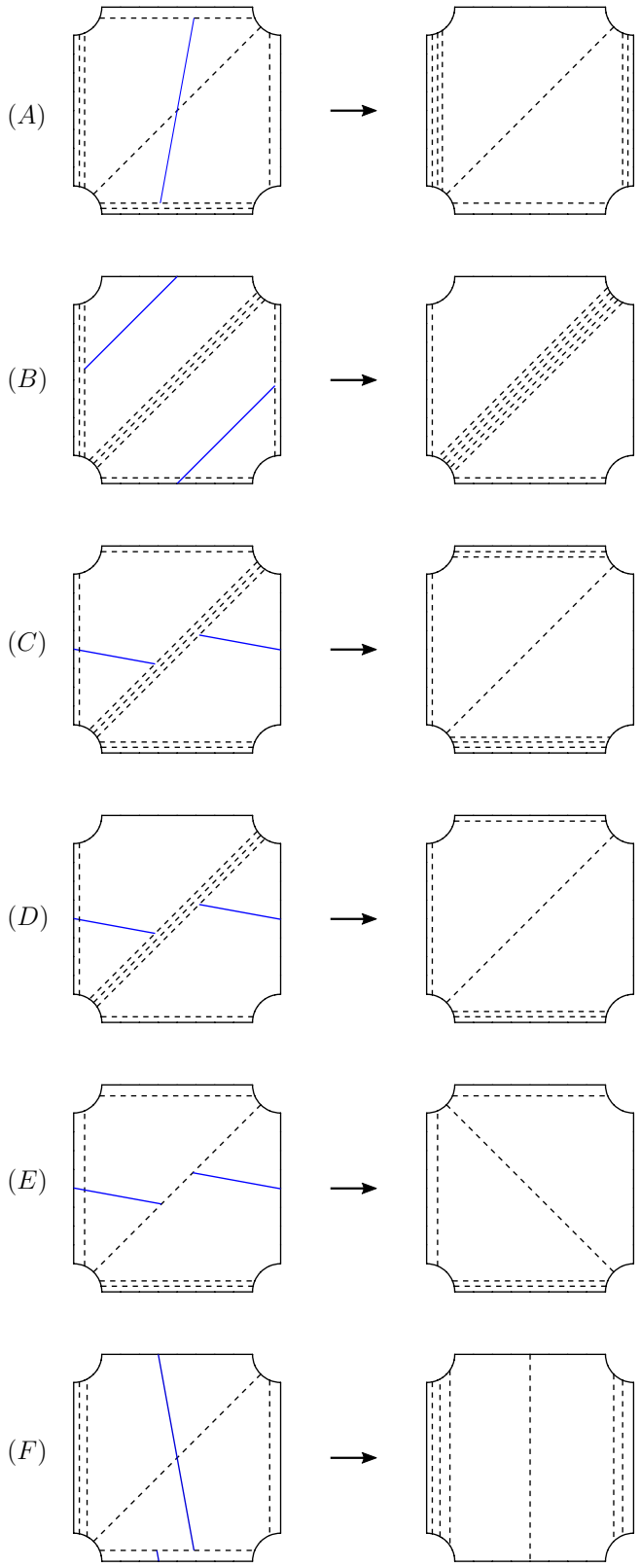

Figure 4.15: List of possible bypass attachments for Case III(a) with $n > 3$. The top and bottom are identified as are the left and right sides. The dashed lines represent dividing curves and the blue solid lines represent the attachment for the bypasses. The bypasses are attached from the back.

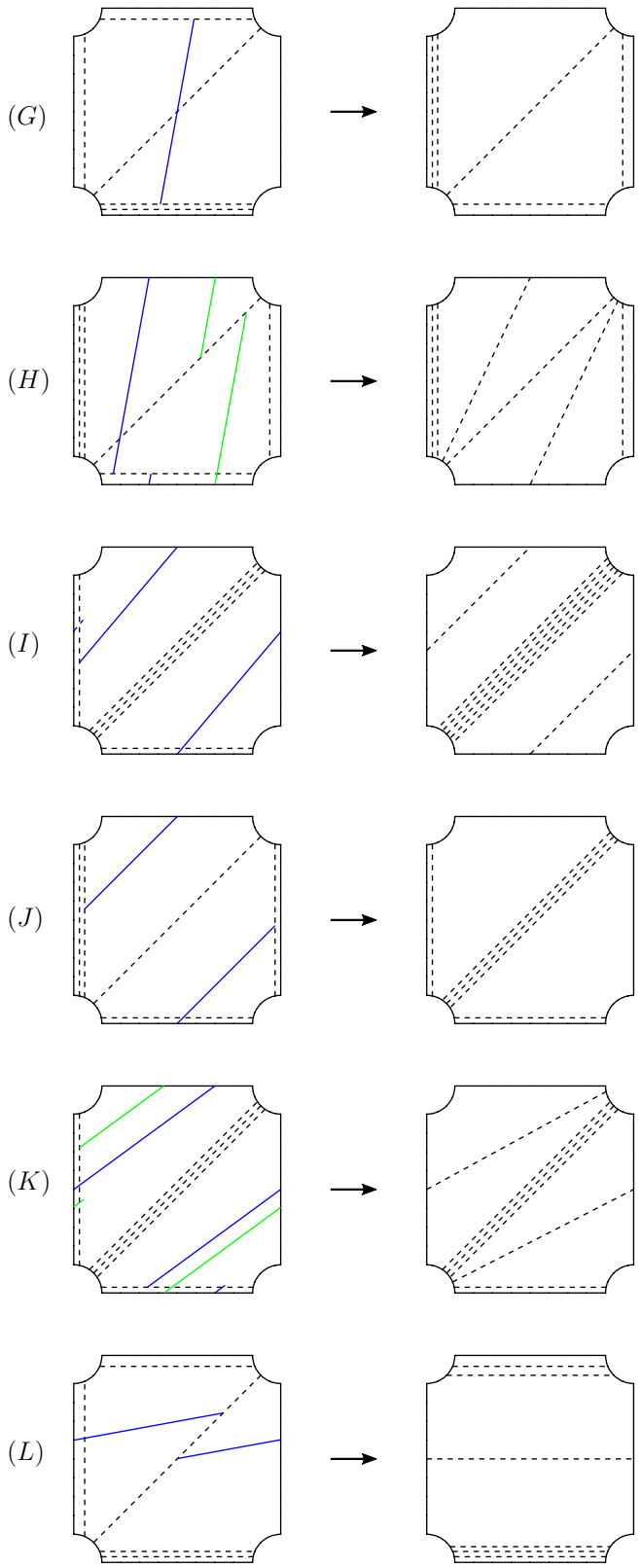

Figure 4.16: Continuation of list of possible bypass attachments for Case III(a) with $n > 3$.

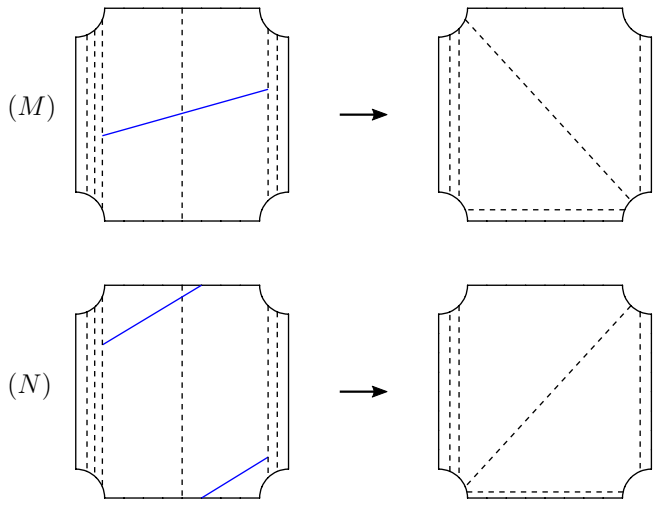

Figure 4.17: Two possible bypass attachments for Case I(a) with $n = 3, m = 1$.

1. $s_1 < s_2 < s_3 \leqslant 0 < p$

2. $0 \leqslant p < s_1 < s_2 < s_3 < \frac{1}{p}$

3. $0 \leqslant s_1 < p < s_2 < s_3 < \frac{1}{p}$ or $0 \leqslant s_1 < s_2 < p < s_3 < \frac{1}{p}$

(1) As discussed above, here we always assume that two isotopy classes have $mult = 1$. We will show that we can perform one of the following moves:

- $\{v_1, v_2, v_3\}$ with $mult(s_2) > 1 \mapsto \{v_1, v_2, v_3\}$ with $mult(s_1) > 1$
- $\{v_1, v_2, v_3\}$ with $mult(s_1) > 1 \mapsto \{v_1, v_2, v_3\}$ with $mult(s_3) > 1$
- $\{v_1, v_2, v_3\}$ with $mult(s_1) > 1 \mapsto \{v_1 - v_3, v_1, v_3\}$ or $\{v_1, v_3, v_3 - v_1\}$
- $\{v_1, v_2, v_3\}$ with $mult(s_3) > 1 \mapsto \{v_3, v_4, v_5\}$: the biggest triangle starting from v_3 in a clockwise direction
- $\{v_1, v_2, v_3\}$ with $mult(s_3) > 1 \mapsto \{\binom{1}{0}\}$

Take an annulus $c \times I$ with slope $\psi(s_3)$. Note that $s_3 \leqslant 0$ and $\psi(s_3) > 0$. Hence, we obtain a bypass of type D, E, F or G. If $mult(s_2) > 1$, the only possible move is of

type D. Apply D once and we obtain C. Apply C repeatedly to make $mult(s_1) > 1$ and $mult(s_2) = 1$. This corresponds to the first move in the above list. If $mult(s_1) > 1$, the only possible moves are E and G. If we have move E, then we can expand the triangle $\{v_1, v_2, v_3\}$ and obtain either $\{v_1 - v_3, v_1, v_3\}$ or $\{v_1, v_3, v_3 - v_1\}$. This corresponds to the third move in the list. If we have move G, apply it once and apply A repeatedly to make $mult(s_3) > 1$ and $mult(s_1) = 1$. This corresponds to the second move in the list. Next, if $mult(s_3) > 1$, apply F and we get $\{v_1, v_2, v_3\} \mapsto \{v_3\}$. Suppose v_3 is not $(\frac{1}{0})$. Take an annulus with slope $\psi(s_3)$ and we obtain a bypass. Let v be the isotopy class with the largest slope for which there exists an edge with v_3 on the Farey graph. Let $v' := v_3 - v$. Take an orientation preserving diffeomorphism of T^2 which sends $\{v', v_3, v\}$ to $\{1, -\infty, 0\}$. Since $\psi(s_3)$ is outside of the triangle $\{v', v_3, v\}$, it lies between $[0, 1]$ after acting via the diffeomorphism. Hence the bypass is of type M or N. M gives $\{v_3\} \mapsto \{v_3, v_3 + v, v\}$, which is the biggest triangle starting from v_3 in a clockwise direction. This corresponds to the fourth move in the list. N gives $\{v_3\} \mapsto \{v', v_3, v\}$, which corresponds to the fourth move followed by the third move in the above list. Thus, we can perform one of the moves in the list by attaching bypasses.

Using the moves in the list, we eventually arrive to $\Gamma_1 = \{-\infty, -1, 0\}$ or $\Gamma_1 = \{0\}$. If $\Gamma_1 = \{0\}$, acting via ψ^{-1} to get $\Gamma_1 = \{\infty\}$. Suppose we have $\Gamma_1 = \{-\infty, -1, 0\}$ with $mult(-1) > 1$. Using the first move in the list, we arrive to $\Gamma_1 = \{-\infty, -1, 0\}$ with $mult(-\infty) > 1$. Take an annulus with slope 0 and we can apply the second move from the list. Hence we arrive to $\Gamma_1 = \{-\infty, -1, 0\}$ with $mult(0) > 1$. Take an annulus with slope $\psi(0) = \frac{1}{3}$ and we can apply the last move in the list. Hence we get $\Gamma_1 = \{0\}$. Acting via ψ^{-1}, we obtain $\Gamma_1 = \{\infty\}$.

(2) After acting via ψ^k, we can further assume that $1 \leqslant s_1 < s_2 < s_3 \leqslant 2$. By the same argument as (1), we eventually arrive to $\Gamma_1 = \{1, \frac{3}{2}, 2\}$ or $\Gamma_1 = \{2\}$. In the former case, take an annulus with the slope $\psi(0) = \frac{1}{3}$ and we obtain a bypass of type E only if $mult(1) > 1$. It changes Γ_1 to $\{1, 2, \infty\}$, which will be dealt with in the case (3). If $mult(1) = 1$, the

bypass gives rise to a bypass along $\partial\Sigma$. If $\Gamma_1 = \{2\}$, act via ψ^{-1} to get $\Gamma_1 = \{1\}$. Take an annulus with slope $\frac{1}{3}$ and we obtain a bypass. This changes Γ_1 to $\{0, \frac{1}{2}, 1\}$, which also will be dealt with in the case (3).

(3) Suppose that we can perform one of the following moves:

- $0 < s_1 < p < s_2 < s_3 < \infty$: $\{v_1, v_2, v_3\}$ with $mult(v_2) > 1 \mapsto \{v_1, v_1 + v_2, v_2\}$ with $mult(v_2) > 1$.
- $0 < s_1 < s_2 < p < s_3 < \infty$: $\{v_1, v_2, v_3\}$ with $mult(v_3) > 1 \mapsto \{v_2, v_2 + v_3, v_3\}$ with $mult(v_3) > 1$.

Using this two moves, we eventually arrive to $\Gamma_1 = \{\psi^k(0), \psi^k(1), \psi^k(\infty)\}$. Note that the actual order is $-\infty < 0 < 1$. Hence we obtain $\Gamma_1 = \{-\infty, 0, 1\}$ with $mult(1) > 1$.

Now we will show that we can perform the moves in the above list or go back to the case (1). First assume $s_1 < s_2 < p < s_3$. Take an annulus with slope $\psi(s_2)$ to find a bypass of type G, H, I or J. I gives $\{v_1, v_2, v_3\} \mapsto \{v_2\}$, so we go back to the case (1). If we have G, then the next move must be H or J. Suppose we have J. Then the next move is I. I gives $\{v_2\}$, so we again go back to the case (1). H gives $\{v_2, v_2 + v_3, v_3\}$ with $mult(v_3) > 1$. Next, suppose $s_1 < p < s_2 < s_3$. Take an annulus with slope $\psi(s_2)$ again to find a bypass of type J, K or L. K gives $\{v_1\}$, so we go back to the case (1). If we have J, the next move must be K, which gives $\{v_1, v_1 + v_2, v_2\}$ with $mult(v_2) > 1$. □

Now we are ready to prove Proposition 4.2.3

Proof of Proposition 4.2.3. By Proposition 4.6.1, we only need to consider the case $\Gamma_1 = \{\infty\}$ or $\Gamma_1 = \{0, 1, \infty\}$ with $mult(0) = mult(\infty) = 1$. The basic strategy of the proof is same as Proposition 4.2.2. First we round edges of $\Sigma \times I$ to make it have a convex boundary. Then, take a convex compressing disk D with Legendrian boundary to find a bypass. We will arrange the disk so that the boundary intersects dividing curves only on Σ_0. As in Proposition 4.2.2, it changes the sides of dividing curves where ∂D is on. Note that there

are $2|5n+2|$ intervals and the slope of dividing curves on $\partial\Sigma \times I$ is $\frac{5n+2}{2n+1}$. This implies that if ∂D is on i-th interval in $\partial\Sigma \times \{0\}$, then ∂D is on $(i - 2|2n+1| - 1) = (i - |4n+1|)$-th interval (mod $2|5n+2|$) in $\partial\Sigma \times \{1\}$.

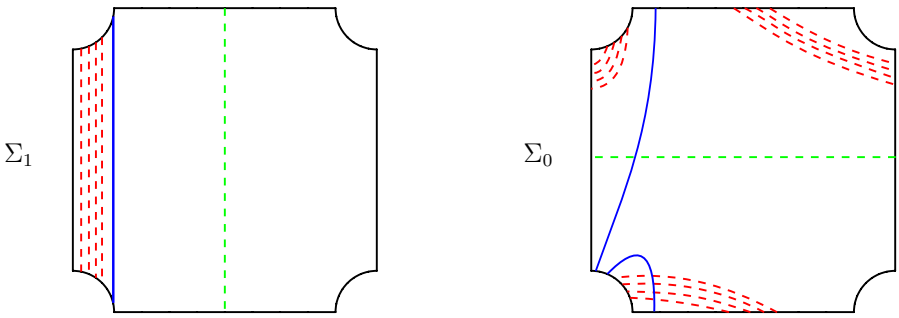

Figure 4.18: The dashed lines represent dividing curves on Σ_1 and Σ_0. The blue solid lines represent the intersection of the compressing disk D with Σ_1 and Σ_0

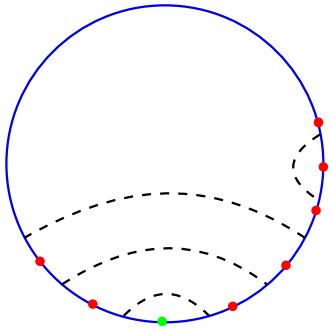

Figure 4.19: The dashed lines represent dividing curves on the compressing disk D. The red dots represent the intersection points of D and the dividing arcs in Γ_0. The green dot represents the intersection point of D and the closed dividing curve in Γ_0.

(1) $\Gamma_1 = \{\infty\}$ and $\Gamma_0 = \{1\}$: Note that curves in Γ_0 are to the right of curves in Γ_1 since ψ is *right-veering*. Take a compressing disk D as shown in Figure 4.18. As discussed above, ∂D intersects dividing curves only on Σ_0 and traverse a closed curve. Above the closed curve, ∂D intersects $|4n+1|$ dividing arcs. Below the closed curve, ∂D intersects $|5n+2| - |4n+1| = |n+1|$ arcs. If $n \leqslant -2$, then $|4n+1| - |n+1| > 1$. This implies that the red dots are not balanced and bypasses cannot be nested with respect to the green dot as shown in Figure 4.19. Hence there exists a bypass on Σ_0 which does not straddle the

green closed dividing curve. This bypass gives rise to a bypass along $\partial\Sigma$.

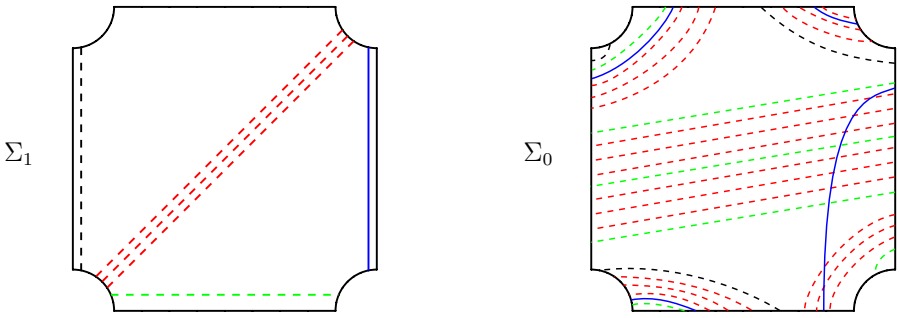

Figure 4.20: The dashed lines represent dividing curves on Σ_1 and Σ_0. The blue solid lines represent the intersection of the compressing disk D with Σ_1 and Σ_0

(2) $\Gamma_1 = \{0, 1, \infty\}$ with $mult(0) = mult(\infty) = 1$ and $\Gamma_0 = \{0, \frac{1}{2}, \frac{1}{3}\}$ with $mult(\frac{1}{3}) = mult(0) = 1$: Take a compressing disk D as shown in Figure 4.20. It is easy to check that ∂D only intersects the red and green dividing curves. The only bypasses which do not give rise to a bypass along $\partial\Sigma$ are bypasses which straddle a green dividing curve. Attaching this bypass yields $\Gamma_0 = \{0, \frac{1}{2}, \frac{1}{3}\}$ with $mult(0) = 3$, $mult(\frac{1}{2}) > 1$ and $mult(\frac{1}{3}) = 1$. Acting via ψ^{-1}, we obtain $\Gamma_1 = \{0, 1, \infty\}$ with $mult(0) = 1$, $mult(1) > 1$ and $mult(\infty) = 3$. Take an annulus with slope 0 and we can find a bypass on Σ_1. Every possible bypass gives rise to a bypass along $\partial\Sigma$.

Hence we can increase the twisting number of L in either case. This completes the proof of Proposition 4.2.3. □

REFERENCES

[1] Y. Eliashberg, "Classification of overtwisted contact structures on 3-manifolds," *Invent. Math.*, vol. 98, no. 3, pp. 623–637, 1989.

[2] Y. Eliashberg, "Contact 3-manifolds twenty years since J. Martinet's work," *Ann. Inst. Fourier (Grenoble)*, vol. 42, no. 1-2, pp. 165–192, 1992.

[3] J. B. Etnyre, "Tight contact structures on lens spaces," *Commun. Contemp. Math.*, vol. 2, no. 4, pp. 559–577, 2000.

[4] E. Giroux, "Structures de contact en dimension trois et bifurcations des feuilletages de surfaces," *Invent. Math.*, vol. 141, no. 3, pp. 615–689, 2000.

[5] K. Honda, "On the classification of tight contact structures. I," *Geom. Topol.*, vol. 4, pp. 309–368, 2000.

[6] J. B. Etnyre and K. Honda, "On the nonexistence of tight contact structures," *Ann. of Math. (2)*, vol. 153, no. 3, pp. 749–766, 2001.

[7] P. Ghiggini and S. Schönenberger, "On the classification of tight contact structures," in *Topology and geometry of manifolds (Athens, GA, 2001)*, ser. Proc. Sympos. Pure Math. Vol. 71, Amer. Math. Soc., Providence, RI, 2003, pp. 121–151.

[8] P. Lisca and A. I. Stipsicz, "On the existence of tight contact structures on Seifert fibered 3-manifolds," *Duke Math. J.*, vol. 148, no. 2, pp. 175–209, 2009.

[9] P. Ghiggini, P. Lisca, and A. I. Stipsicz, "Tight contact structures on some small Seifert fibered 3-manifolds," *Amer. J. Math.*, vol. 129, no. 5, pp. 1403–1447, 2007.

[10] Y. Kanda, "The classification of tight contact structures on the 3-torus," *Comm. Anal. Geom.*, vol. 5, no. 3, pp. 413–438, 1997.

[11] E. Giroux, "Une infinité de structures de contact tendues sur une infinité de variétés," *Invent. Math.*, vol. 135, no. 3, pp. 789–802, 1999.

[12] ——, "Structures de contact sur les variétés fibrées en cercles audessus d'une surface," *Comment. Math. Helv.*, vol. 76, no. 2, pp. 218–262, 2001.

[13] K. Honda, "On the classification of tight contact structures. II," *J. Differential Geom.*, vol. 55, no. 1, pp. 83–143, 2000.

[14] K. Honda, W. H. Kazez, and G. Matić, "Convex decomposition theory," *Int. Math. Res. Not.*, no. 2, pp. 55–88, 2002.

[15] V. Colin, E. Giroux, and K. Honda, "Finitude homotopique et isotopique des structures de contact tendues," *Publ. Math. Inst. Hautes Études Sci.*, no. 109, pp. 245–293, 2009.

[16] K. Honda, W. H. Kazez, and G. Matić, "Tight contact structures on fibered hyperbolic 3-manifolds," *J. Differential Geom.*, vol. 64, no. 2, pp. 305–358, 2003.

[17] J. Conway and H. Min, "Classification of tight contact structures on surgeries on the figure-eight knot," *Geom. Topol.*, vol. 24, no. 3, pp. 1457–1517, 2020.

[18] D. Gabai, R. Meyerhoff, and P. Milley, "Minimum volume cusped hyperbolic three-manifolds," *J. Amer. Math. Soc.*, vol. 22, no. 4, pp. 1157–1215, 2009.

[19] K. Honda, "The topology and geometry of contact structures in dimension three," in *International Congress of Mathematicians. Vol. II*, Eur. Math. Soc., Zürich, 2006, pp. 705–717.

[20] T. Etgü, "Tight contact structures on laminar free hyperbolic three-manifolds," *Int. Math. Res. Not. IMRN*, no. 20, pp. 4775–4784, 2012.

[21] A. I. Stipsicz, "Tight contact structures on the Weeks manifold," *Proceedings of Gökova Geometry-Topology Conference 2007*, pp. 82–89, 2008.

[22] J. B. Etnyre, "Legendrian and transversal knots," in *Handbook of knot theory*, Elsevier B. V., Amsterdam, 2005, pp. 105–185.

[23] ——, "Introductory lectures on contact geometry," *Proc. Sympos. Pure Math.*, vol. 71, pp. 81–107, 2003.

[24] ——, "Convex surfaces in contact geometry: Class notes," in.

[25] E. Giroux, "Convexité en topologie de contact," *Comment. Math. Helv.*, vol. 66, no. 4, pp. 637–677, 1991.

[26] F. Ding and H. Geiges, "A Legendrian surgery presentation of contact 3-manifolds," *Math. Proc. Cambridge Philos. Soc.*, vol. 136, no. 3, pp. 583–598, 2004.

[27] F. Ding, H. Geiges, and A. I. Stipsicz, "Surgery diagrams for contact 3-manifolds," *Turkish J. Math.*, vol. 28, no. 1, pp. 41–74, 2004.

[28] P. Ozsváth and Z. Szabó, "Holomorphic disks and topological invariants for closed three-manifolds," *Ann. of Math. (2)*, vol. 159, no. 3, pp. 1027–1158, 2004.

[29] ——, "Holomorphic disks and three-manifold invariants: Properties and applications," *Ann. of Math. (2)*, vol. 159, no. 3, pp. 1159–1245, 2004.

[30] ——, "Heegaard Floer homology and contact structures," *Duke Math. J.*, vol. 129, no. 1, pp. 39–61, 2005.

[31] P. Lisca and A. I. Stipsicz, "Ozsváth-Szabó invariants and tight contact three-manifolds. I," *Geom. Topol.*, vol. 8, pp. 925–945, 2004.

[32] R. E. Gompf, "Handlebody construction of Stein surfaces," *Ann. of Math. (2)*, vol. 148, no. 2, pp. 619–693, 1998.

[33] C. D. Hodgson, G. R. Meyerhoff, and J. R. Weeks, "Surgeries on the Whitehead link yield geometrically similar manifolds," *Topology '90 (Columbus, OH, 1990)*, vol. 1, pp. 195–206, 1992.

[34] K. Morimoto, "Genus one fibered knots in lens spaces," *J. Math. Soc. Japan*, vol. 41, no. 1, pp. 81–96, 1989.

[35] J. B. Etnyre and K. Honda, "Knots and contact geometry. I. Torus knots and the figure eight knot," *J. Symplectic Geom.*, vol. 1, no. 1, pp. 63–120, 2001.

[36] K. Honda, W. H. Kazez, and G. Matić, "Right-veering diffeomorphisms of compact surfaces with boundary," *Invent. Math.*, vol. 169, no. 2, pp. 427–449, 2007.

[37] J. Conway, "Contact surgeries on the legendrian figure-eight knot," *arXiv preprint arXiv:1610.03943*, 2016.